B-meson observables in the maximally *CP*-violating MSSM with minimal flavor violation

John Ellis,[1] Jae Sik Lee,[2] and Apostolos Pilaftsis[1,3]

[1]*Theory Division, Physics Department, CERN, CH-1211 Geneva 23, Switzerland*
[2]*Center for Theoretical Physics, School of Physics, Seoul National University, Seoul 151-747, Korea*
[3]*School of Physics and Astronomy, University of Manchester, Manchester M13 9PL, United Kingdom*

(Received 22 August 2007; published 18 December 2007)

Additional sources of *CP* violation in the MSSM may affect *B*-meson mixings and decays, even in scenarios with minimal flavor violation (MFV). We formulate the maximally *CP*-violating and minimally flavor-violating (MCPMFV) variant of the MSSM, which has 19 parameters, including 6 phases that violate *CP*. We then develop a manifestly flavor-covariant effective Lagrangian formalism for calculating Higgs-mediated flavor-changing-neutral-current (FCNC) observables in the MSSM at large $\tan\beta$, and analyze within the MCPMFV framework FCNC and other processes involving *B* mesons. We include a new class of dominant subleading contributions due to nondecoupling effects of the third-generation quarks. We present illustrative numerical results that include effects of the *CP*-odd MCPMFV parameters on Higgs and sparticle masses, the B_s and B_d mass differences, and on the decays $B_s \to \mu^+\mu^-$, $B_u \to \tau\nu$, and $b \to s\gamma$. We use these results to derive illustrative constraints on the MCPMFV parameters imposed by D0, CDF, Belle, and *BABAR* measurements of *B* mesons, demonstrating how a potentially observable contribution to the *CP* asymmetry in the $b \to s\gamma$ decay may arise in the MSSM with MCPMFV.

DOI: 10.1103/PhysRevD.76.115011 PACS numbers: 12.60.Jv, 13.20.He

I. INTRODUCTION

Models incorporating supersymmetry (SUSY), such as the minimal supersymmetric standard model (MSSM), contain many possible sources of flavor and *CP* violation. In particular, the soft SUSY-breaking sector in general introduces many new sources of flavor and *CP* violation, giving rise to effects that may exceed the experimental limits by several orders of magnitude. The unitarity of the Cabibbo-Kobayashi-Maskawa (CKM) quark mixing matrix suppresses flavor-changing-neutral currents (FCNC) and *CP* violation somewhat, thanks to the Glashow-Iliopoulos-Maiani (GIM) mechanism [1], to the extent that the soft SUSY-breaking scalar masses are universal. One possible solution to the flavor and *CP* problems is to ensure that the soft SUSY-breaking sector is fully protected by the GIM mechanism. This can be achieved within the so-called framework of minimal flavor violation (MFV), where all flavor and *CP* effects are mediated by the superpotential interactions corresponding to the ordinary Yukawa couplings of the Higgs bosons to quarks and leptons. In this framework, FCNC and *CP*-violating observables depend only on the fermion masses and their mixings, and hence the CKM mixing matrix $\mathbf{V}$ [2]. In such a scenario, all FCNC and *CP*-violation observables would vanish in the MSSM if $\mathbf{V}$ were equal to the unit matrix $\mathbf{1}$.

A minimal realization of MFV in the MSSM is obtained by assuming that all soft SUSY-breaking bilinear masses for the scalar particles, such as squarks, sleptons, and Higgs bosons, are equal to a common value m_0 at the gauge coupling unification point $M_{\rm GUT}$, where $M_{\rm GUT}$ might be the threshold for some underlying grand unified theory (GUT) based, e.g., on SU(5) or SO(10). Likewise, the soft masses of the fermionic SUSY partners of the gauge fields, the gauginos, might also be equal to a common value $m_{1/2}$ at $M_{\rm GUT}$ and, in the same spirit, all soft trilinear Yukawa couplings of the Higgs bosons to squarks and sleptons could be real and equal to a universal parameter *A* times the corresponding Higgs-fermion-antifermion couplings. The Higgs supermultiplet mixing parameter μ and the corresponding soft SUSY-breaking term $B\mu$ introduce two additional mass scales in the theory. However, minimization conditions on the Higgs potential can be used to eliminate these two last mass scales in favor of the electroweak scale M_Z and $\tan\beta \equiv v_u/v_d$, where $v_{u,d}$ are the vacuum expectation values (VEVs) of the two Higgs doublets $H_{u,d}$ in the MSSM.

It is well known that a minimal expansion of the above MFV framework is to allow the soft SUSY-breaking mass parameters $m_{1/2}$ and *A* to be complex with *CP*-odd phases, thereby introducing two additional sources of *CP* violation in the theory. In this case, all FCNC observables, whether *CP* conserving or not, still depend on the CKM mixing matrix $\mathbf{V}$ in such a way that they vanish if $\mathbf{V}$ is assumed to be diagonal, i.e., equal to the unit matrix. However, the two new phases introduce the possibility of *CP* violation in flavor-conserving processes even if $\mathbf{V}$ is real, and in general *CP* violation in FCNC processes may differ from CKM predictions.

Here we go one step further, and ask the following question. What is the maximal number of additional *CP*-violating parameters and extra flavor-singlet mass scales that could be present in the MSSM, for which the above notion of MFV remains still valid, i.e., all FCNC

effects vanish in the limit of a diagonal **V**? We call this scenario the maximally *CP*-violating MSSM with minimal flavor violation, or in short, the MSSM with MCPMFV. As we will see in Sec. II, there are a total of 19 parameters in the MSSM with MCPMFV, including 6 *CP*-violating phases and 13 real mass parameters. The purposes of this paper are to formulate the MSSM with MCPMFV, calculate the most relevant B-meson observables, and explore the experimental constraints on the MCPMFV theoretical parameters, exploiting a manifestly flavor-covariant effective Lagrangian formalism for calculating Higgs-mediated FCNC observables at large $\tan\beta$ that we develop here.

At large values of $\tan\beta$, e.g. $\tan\beta \gtrsim 40$, one-loop threshold effects on Higgs-boson interactions to down-type quarks get enhanced [3–5], and so play an important role in FCNC processes, such as the K^0-$\bar{K}^0$ mass difference, B_s-$\bar{B}_s$ and B_d-$\bar{B}_d$ mixings, and the decays $B \to X_s\gamma$, $B \to Kl^+l^-$, $B_{s,d} \to \mu^+\mu^-$ [6–15], and $B \to \tau\nu$ [16,17]. We present in this paper a manifestly flavor-covariant effective Lagrangian formalism for calculating FCNC processes that follows the lines of the effective Lagrangian approach given in [12]. In addition, we include here the dominant subleading contributions to the one-loop Higgs-mediated FCNC interactions due to nondecoupling large Yukawa-coupling effects of the third-generation quarks. Based on this improved formalism, we compute FCNC observables in constrained versions of the MSSM, where MFV has been imposed on the soft SUSY-breaking mass parameters as a boundary condition at the scale $M_{\rm GUT}$. We present numerical results for B-meson observables in one example of the MCPMFV framework, from which illustrative constraints on the basic theoretical parameters are derived, after incorporating the recent experimental results from D0 and CDF [18].

The paper is organized as follows: in Sec. II, after briefly reviewing the MFV framework, we derive the maximal number of flavour-singlet mass parameters that can be present in the MSSM with MCPMFV at the GUT scale. All relevant one-loop renormalization group equations (RGEs) are given in Appendix A. In Sec. III, we present an effective Lagrangian formalism for Higgs-mediated FCNC interactions that respects flavor covariance. We also discuss the dominant subleading effects at large $\tan\beta$, due to the large Yukawa couplings of the third generation. Useful relations which result from Ward identities (WIs) that involve the Z and W-boson interactions to quarks are derived in Appendix B. Section IV summarizes all relevant analytic results pertinent to FCNC B-meson observables. In Sec. V we exhibit numerical estimates and predictions for various FCNC processes, including the B_s-$\bar{B}_s$ and B_d-$\bar{B}_d$ mixings, and the decays $B_{s,d} \to \mu^+\mu^-$, $B \to X_s\gamma$, and $B \to \tau\nu$. We also illustrate the combined constraints on the theoretical parameters imposed by data from D0, CDF, Belle, and *BABAR* in one sample MCPMFV model. We summarize our conclusions in Sec. VI.

II. MAXIMAL *CP* AND MINIMAL FLAVOR VIOLATION

In this section we derive the maximal number of *CP*-violating and real flavor-singlet mass parameters that can be present in the *CP*-violating MSSM and satisfy the property of MFV as described in the introduction.

The superpotential defining the flavor structure of the MSSM may be written as

$$W_{\rm MSSM} = \hat{U}^C \mathbf{h}_u \hat{Q} \hat{H}_u + \hat{D}^C \mathbf{h}_d \hat{H}_d \hat{Q} + \hat{E}^C \mathbf{h}_e \hat{H}_d \hat{L} + \mu \hat{H}_u \hat{H}_d, \tag{2.1}$$

where $\hat{H}_{u,d}$ are the two Higgs chiral superfields, and $\hat{Q}$, $\hat{L}$, $\hat{U}^C$, $\hat{D}^C$, and $\hat{E}^C$ are the left- and right-handed superfields related to up- and down-type quarks and charged leptons. The Yukawa couplings $\mathbf{h}_{u,d,e}$ are 3×3 complex matrices describing the charged-lepton and quark masses and their mixings. The superpotential (2.1) contains one mass parameter, the μ parameter that mixes the Higgs supermultiplets, which has to be of the electroweak order for a natural realization of the Higgs mechanism.

In an unconstrained version of the MSSM, there is a large number of different mass parameters present in the soft SUSY-breaking Lagrangian

$$\begin{aligned} -\mathcal{L}_{\rm soft} = {} & \tfrac{1}{2}(M_1 \tilde{B}\tilde{B} + M_2 \tilde{W}^i \tilde{W}^i + M_3 \tilde{g}^a \tilde{g}^a + \text{H.c.}) \\ & + \tilde{Q}^\dagger \tilde{\mathbf{M}}_Q^2 \tilde{Q} + \tilde{L}^\dagger \tilde{\mathbf{M}}_L^2 \tilde{L} + \tilde{U}^\dagger \tilde{\mathbf{M}}_U^2 \tilde{U} + \tilde{D}^\dagger \tilde{\mathbf{M}}_D^2 \tilde{D} \\ & + \tilde{E}^\dagger \tilde{\mathbf{M}}_E^2 \tilde{E} + M_{H_u}^2 H_u^\dagger H_u + M_{H_d}^2 H_d^\dagger H_d \\ & + (B\mu H_u H_d + \text{H.c.}) \\ & + (\tilde{U}^\dagger \mathbf{a}_u \tilde{Q} H_u + \tilde{D}^\dagger \mathbf{a}_d H_d \tilde{Q} + \tilde{E}^\dagger \mathbf{a}_e H_d \tilde{L} + \text{H.c.}). \end{aligned} \tag{2.2}$$

Here $M_{1,2,3}$ are the soft SUSY-breaking masses associated with the $\mathrm{U}(1)_Y$, $\mathrm{SU}(2)_L$, and $\mathrm{SU}(3)_c$ gauginos, respectively. In addition, $M_{H_{u,d}}^2$ and $B\mu$ are the soft masses related to the Higgs doublets $H_{u,d}$ and their bilinear mixing. Finally, $\tilde{\mathbf{M}}_{Q,L,D,U,E}^2$ are the 3×3 soft mass-squared matrices of squarks and sleptons, and $\mathbf{a}_{u,d,e}$ are the corresponding 3×3 soft Yukawa mass matrices.[1] Hence, in addition to the μ term, the unconstrained *CP*-violating MSSM contains 109 real mass parameters.

One frequently considers the constrained MSSM (CMSSM), which has a common gaugino mass $m_{1/2}$, a common soft SUSY-breaking scalar mass m_0 and a common soft trilinear Yukawa coupling A for all squarks and sleptons at the GUT scale. The number of independent

[1]Alternatively, the soft Yukawa mass matrices $\mathbf{a}_{u,d,e}$ may be defined by the relation: $(\mathbf{a}_{u,d,e})_{ij} = (\mathbf{h}_{u,d,e})_{ij}(\mathbf{A}_{u,d,e})_{ij}$, where the parameters $(\mathbf{A}_{u,d,e})_{ij}$ are generically of order $M_{\rm SUSY}$ in gravity-mediated SUSY-breaking models. In our paper, both definitions for the soft SUSY-breaking Yukawa couplings will be used, where convenient.

mass scales is greatly reduced since, even allowing for maximal *CP* violation, the free parameters are just $m_{1/2}$, μ, m_0, A, and $B\mu$, where all but m_0 are complex variables. The phase $\arg\mu$ may be removed by means of a global Peccei-Quinn (PQ) symmetry under which H_u and H_d have the same charges. Imposing the two *CP*-even tadpole conditions on the Higgs potential, one may replace $\mu = |\mu|$ and $\mathrm{Re}(B\mu)$ by the Z-boson mass M_Z and the ratio $\tan\beta = v_u/v_d$ of the VEVs of the Higgs doublets $H_{u,d}$, in the phase convention where $v_{u,d}$ are real and positive. Linked to this, there is one extra *CP*-odd tadpole condition which can be used to eliminate $\mathrm{Im}(B\mu)$ in favor of maintaining the same phase convention for the VEVs, order by order in perturbation theory [19]. Thus, a convenient set of input mass parameters of the constrained *CP*-violating MSSM is

$$\begin{aligned} &\tan\beta(m_t), \qquad m_{1/2}(M_{\mathrm{GUT}}),\\ &m_0(M_{\mathrm{GUT}}), \qquad A(M_{\mathrm{GUT}}), \end{aligned} \tag{2.3}$$

where the relative sign of μ can always be absorbed into the phase definition of the complex parameters $m_{1/2}$ and A. Thus, in addition to $\tan\beta$, this *CP*-violating CMSSM has just 5 real mass parameters, two more than in its *CP*-conserving counterpart, namely, the *CP*-odd parameters: $\mathrm{Im}\, m_{1/2}$ and $\mathrm{Im}\, A$.

How can the general notion of MFV be extended to this constrained *CP*-violating MSSM? In such a constrained model, the physical FCNC observables remain independent of details of the Yukawa texture chosen at the GUT scale. They depend only on the CKM mixing matrix $\mathbf{V}$, the fermion masses, $\tan\beta$, and the 5 real mass parameters mentioned above. If the CKM matrix $\mathbf{V}$ were equal to the unit matrix $\mathbf{1}$, the FCNC observables would vanish, but flavor-conserving, *CP*-violating effects would still be present, associated with $\mathrm{Im}\, m_{1/2}$ and $\mathrm{Im}\, A$. Moreover, these parameters also contribute to *CP*-violating FCNC observables in the presence of nontrivial CKM mixing. Most noticeably, $\mathrm{Im}\, m_{1/2}$ and $\mathrm{Im}\, A$ cannot generically mimic the effects of the usual CKM phase δ.

We now consider how the above notion of MFV can be further extended within the more general *CP*-violating MSSM. To address this question, we first notice that under the unitary flavor rotations of the quark and lepton superfields,

$$\begin{aligned} &\hat{Q}' = \mathbf{U}_Q\hat{Q}, \qquad \hat{L}' = \mathbf{U}_L\hat{L}, \qquad \hat{U}'^C = \mathbf{U}_U^*\hat{U}^C,\\ &\hat{D}'^C = \mathbf{U}_D^*\hat{D}^C, \qquad \hat{E}'^C = \mathbf{U}_E^*\hat{E}^C, \end{aligned} \tag{2.4}$$

the complete MSSM Lagrangian of the theory remains invariant provided the model parameters are redefined as follows:

$$\begin{aligned} \mathbf{h}_{u,d} &\to \mathbf{U}_{U,D}^\dagger \mathbf{h}_{u,d}\mathbf{U}_Q,\\ \mathbf{h}_e &\to \mathbf{U}_E^\dagger \mathbf{h}_e \mathbf{U}_L,\\ \tilde{\mathbf{M}}^2_{Q,L,U,D,E} &\to \mathbf{U}^\dagger_{Q,L,U,D,E}\tilde{\mathbf{M}}^2_{Q,L,U,D,E}\mathbf{U}_{Q,L,U,D,E},\\ \mathbf{a}_{u,d} &\to \mathbf{U}_{U,D}^\dagger \mathbf{a}_{u,d}\mathbf{U}_Q,\\ \mathbf{a}_e &\to \mathbf{U}_E^\dagger \mathbf{a}_e \mathbf{U}_L. \end{aligned} \tag{2.5}$$

The remaining mass scales, μ, $M_{1,2,3}$, $M^2_{H_{u,d}}$, and $B\mu$, do not transform under the unitary flavor rotations (2.4). In fact, it is apparent that the one-loop RGEs presented in Appendix A are invariant under the redefinitions in (2.5), provided the unitary flavor matrices $\mathbf{U}_{Q,L,U,D,E}$ are taken to be independent of the RG scale. The effective Lagrangian formalism we describe in Sec. III respects manifestly the property of flavor covariance under the unitary transformations (2.4).

It is apparent from (2.5) that the maximal set of flavor-singlet mass scales includes:

$$\begin{aligned} &M_{1,2,3}, \qquad M^2_{H_{u,d}}, \qquad \tilde{\mathbf{M}}^2_{Q,L,U,D,E} = \tilde{M}^2_{Q,L,U,D,E}\mathbf{1}_3,\\ &\mathbf{A}_{u,d,e} = A_{u,d,e}\mathbf{1}_3, \end{aligned} \tag{2.6}$$

where the mass parameters μ and $B\mu$ can be eliminated by virtue of a global PQ symmetry and by the *CP*-even and *CP*-odd minimization conditions on the Higgs potential. The scenario (2.6) has a total of 19 mass parameters that respect the general MFV property, 6 of which are *CP* odd, namely $\mathrm{Im}\, M_{1,2,3}$ and $\mathrm{Im}A_{u,d,e}$.

We term this scenario the maximally CP-violating and minimally flavor-violating (MCPMFV) variant of the MSSM, or in short, the MSSM with MCPMFV.

It is worth noting that, in addition to the flavor-singlet mass scales mentioned above, there may exist flavor *nonsinglet* mass scales in the MSSM. For example, one could impose an unconventional boundary condition on the left-handed squark mass matrix $\tilde{\mathbf{M}}^2_Q$, such that

$$\begin{aligned} \tilde{\mathbf{M}}^2_Q(M_X) = \tilde{M}^2_Q\mathbf{1}_3 + \tilde{m}^2_1(\mathbf{h}_d^\dagger\mathbf{h}_d) + \tilde{m}^2_2(\mathbf{h}_u^\dagger\mathbf{h}_u)\\ + \tilde{m}^2_3(\mathbf{h}_d^\dagger\mathbf{h}_d)(\mathbf{h}_u^\dagger\mathbf{h}_u) + \ldots, \end{aligned} \tag{2.7}$$

where M_X could be M_{GUT} or some other scale. Evidently, there are in principle a considerable number of extra mass parameters $\tilde{m}^2_n$ that could also be present in $\tilde{\mathbf{M}}^2_Q(M_X)$, beyond the flavor-singlet mass scale $\tilde{M}^2_Q$. In fact, these additional flavor nonsinglet mass parameters $\tilde{m}^2_n$ can be as many as 9 (including $\tilde{M}^2_Q$), as determined by the dimensionality of the 3×3 Hermitian matrix $\tilde{\mathbf{M}}^2_Q(M_X)$. The generalized boundary condition (2.7) on $\tilde{\mathbf{M}}^2_Q(M_X)$ is in agreement with the notion of MFV for solving the flavor problem by suppressing the GIM-breaking effects, provided the hierarchy $\tilde{m}^2_n \ll \tilde{M}^2_Q$ is assumed. In particular, if these flavor-nonsinglet mass parameters $\tilde{m}^2_n$ are induced by RG running, they may be generically much smaller than

$\tilde{M}_Q^2$. In this case, the $\tilde{m}_n^2$ will not all be independent of each other, e.g., in our MCPMFV scenario, the RG-induced flavor-nonsinglet scales $\tilde{m}_n^2$ would be functionals of the 19 flavor-singlet mass parameters stated in (2.6). In general, a nonsinglet mass parameter could either be introduced by hand or induced by RG running of a theory beyond the MSSM with more flavor-singlet mass scales [20]. However, since introducing $\tilde{m}_n^2 \ll \tilde{M}_Q^2$ by hand has no strong theoretical motivation, we focus our attention here on the flavor-singlet MSSM framework embodied by the MCPMFV.

Before calculating FCNC observables in the MSSM with MCPMFV, we first develop in the next section an effective Lagrangian approach to the computation of Higgs-mediated effects, which play an important role in our analysis.

III. EFFECTIVE LAGRANGIAN FORMALISM

Here we present a manifestly flavor-covariant effective Lagrangian formalism. This formalism enables one to show the flavor-basis independence of FCNC observables in general soft SUSY-breaking scenarios of the MSSM. It will also be used in Sec. IV to calculate FCNC processes in the MSSM with MCPMFV.

To make contact between our notation and that used elsewhere in the literature [21], we redefine the Higgs doublets $H_{u,d}$ as $H_u \equiv \Phi_2$ and $H_d \equiv i\tau_2\Phi_1^*$, where τ_2 is the usual antisymmetric Pauli matrix. We start our discussion by considering the effective Lagrangian that describes the $\tan\beta$-enhanced supersymmetric contributions to the down-type quark self-energies as shown in Fig. 1. The effective Lagrangian can be written in gauge-symmetric and flavor-covariant form as follows:

$$-\mathcal{L}_{\rm eff}^{d}[\Phi_1,\Phi_2] = \bar{d}^0_{iR}(\mathbf{h}_d\Phi_1^\dagger + \Delta\mathbf{h}_d[\Phi_1,\Phi_2])_{ij}Q^0_{jL} + \text{H.c.}, \tag{3.1}$$

where the superscript "0" indicates weak-eigenstate fields. In (3.1), the first term denotes the tree-level contribution and $\Delta\mathbf{h}_d$ is a 3×3 matrix which is a Coleman-Weinberg-type [22] effective functional of the background Higgs doublets $\Phi_{1,2}$. We note that the one-loop effective functional $\Delta\mathbf{h}_d[\Phi_1,\Phi_2]$ has the same gauge and flavor transformation properties as $\mathbf{h}_d\Phi_1^\dagger$. Its analytic and flavor-covariant form may be calculated via

$$\begin{aligned}(\Delta\mathbf{h}_d)_{ij} = \int \frac{d^nk}{(2\pi)^n i}\Bigg[& P_L\frac{M_3^*}{k^2-|M_3^2|}\left(\frac{1}{k^2\mathbf{1}_{12}-\tilde{\mathbf{M}}^2}\right)_{\tilde{D}_i\tilde{Q}_j^\dagger} \\ & + P_L\left(\frac{1}{\not{k}\mathbf{1}_8 - \mathbf{M}_C P_L - \mathbf{M}_C^\dagger P_R}\right)_{\tilde{H}_u\tilde{H}_d} \\ & \times P_L(\mathbf{h}_d)_{il}\left(\frac{1}{k^2\mathbf{1}_{12}-\tilde{\mathbf{M}}^2}\right)_{\tilde{Q}_l\tilde{U}_k^\dagger}(\mathbf{h}_u)_{kj} \\ & + P_L\left(\frac{1}{\not{k}\mathbf{1}_8 - \mathbf{M}_C P_L - \mathbf{M}_C^\dagger P_R}\right)_{\tilde{H}_d\tilde{W}^k,\tilde{H}_d\tilde{B}} \\ & \times P_L(\mathbf{h}_d)_{il}\left(\frac{1}{k^2\mathbf{1}_{12}-\tilde{\mathbf{M}}^2}\right)_{\tilde{Q}_l\tilde{Q}_j^\dagger}\Bigg],\end{aligned} \tag{3.2}$$

where $n = 4-2\epsilon$ is the usual number of analytically continued dimensions in dimensional regularization (DR), $\mathbf{1}_N$ stands for the $N\times N$-dimensional unit matrix, and $P_{L(R)} = \frac{1}{2}[1-(+)\gamma_5]$ are the standard chirality-projection operators. The 8×8- and 12×12-dimensional matrices $\mathbf{M}_C$ and $\tilde{\mathbf{M}}^2$ describe the squark and chargino-neutralino mass spectrum in the background of nonvanishing Higgs doublets $\Phi_{1,2}$.

It proves convenient to express the 8×8-dimensional chargino-neutralino mass matrix $\mathbf{M}_C$ in the Weyl basis $(\tilde{B}, \tilde{W}^{1,2,3}, \tilde{H}_u, \tilde{H}_d)$, where $\tilde{H}_{u,d}$ are SU(2)$_L$ doublets: $\tilde{H}_u = (\tilde{h}_u^+, \tilde{h}_u^0)^T$ and $\tilde{H}_d = (\tilde{h}_d^0, \tilde{h}_d^-)^T$. In this weak basis, the Higgs-field-dependent chargino-neutralino mass matrix $\mathbf{M}_C[\Phi_1,\Phi_2]$ reads:

$$\mathbf{M}_C[\Phi_1,\Phi_2] = \begin{pmatrix} M_1 & 0 & -\frac{1}{\sqrt{2}}g'\Phi_2^\dagger & \frac{1}{\sqrt{2}}g'\Phi_1^T(i\tau_2) \\ 0 & M_2\mathbf{1}_3 & \frac{1}{\sqrt{2}}g\Phi_2^\dagger\tau_i & -\frac{1}{\sqrt{2}}g\Phi_1^T(i\tau_2)\tau_i \\ -\frac{1}{\sqrt{2}}g'\Phi_2^* & \frac{1}{\sqrt{2}}g\tau_i^T\Phi_2^* & \mathbf{0}_2 & \mu(i\tau_2) \\ -\frac{1}{\sqrt{2}}(i\tau_2)g'\Phi_1 & \frac{1}{\sqrt{2}}g\tau_i^T(i\tau_2)\Phi_1 & -\mu(i\tau_2) & \mathbf{0}_2 \end{pmatrix}, \tag{3.3}$$

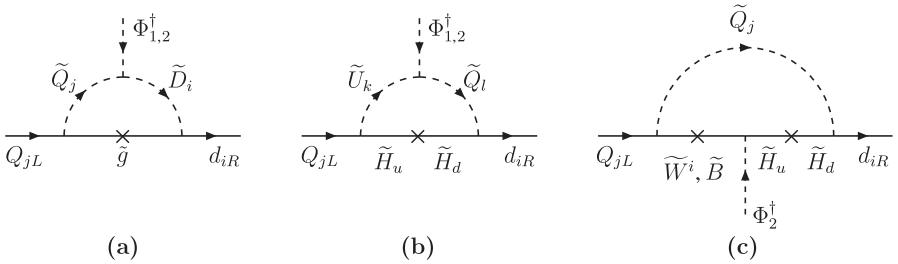

(a) (b) (c)

FIG. 1. Gauge- and flavor-invariant one-loop self-energy graphs for down-type quarks in the single-Higgs insertion approximation, with $H_u \equiv \Phi_2$ and $H_d \equiv i\tau_2\Phi_1^*$.

where g and g' are the $SU(2)_L$ and $U(1)_Y$ gauge couplings, respectively. Correspondingly, in the presence of nonvanishing Higgs doublets $\Phi_{1,2}$, the 12×12-dimensional squark mass matrix $\tilde{\mathbf{M}}^2[\Phi_1, \Phi_2]$ is given by

$$\tilde{\mathbf{M}}^2[\Phi_1, \Phi_2] = \begin{pmatrix} (\tilde{\mathbf{M}}^2)_{\tilde{Q}^\dagger \tilde{Q}} & (\tilde{\mathbf{M}}^2)_{\tilde{Q}^\dagger \tilde{U}} & (\tilde{\mathbf{M}}^2)_{\tilde{Q}^\dagger \tilde{D}} \\ (\tilde{\mathbf{M}}^2)_{\tilde{U}^\dagger \tilde{Q}} & (\tilde{\mathbf{M}}^2)_{\tilde{U}^\dagger \tilde{U}} & (\tilde{\mathbf{M}}^2)_{\tilde{U}^\dagger \tilde{D}} \\ (\tilde{\mathbf{M}}^2)_{\tilde{D}^\dagger \tilde{Q}} & (\tilde{\mathbf{M}}^2)_{\tilde{D}^\dagger \tilde{U}} & (\tilde{\mathbf{M}}^2)_{\tilde{D}^\dagger \tilde{D}} \end{pmatrix}_{ij}, \tag{3.4}$$

with

$$\begin{aligned}
(\tilde{\mathbf{M}}^2)_{\tilde{Q}_i^\dagger \tilde{Q}_j} &= (\tilde{\mathbf{M}}_Q^2)_{ij} \mathbf{1}_2 + (\mathbf{h}_d^\dagger \mathbf{h}_d)_{ij} \Phi_1 \Phi_1^\dagger + (\mathbf{h}_u^\dagger \mathbf{h}_u)_{ij} (\Phi_2^\dagger \Phi_2 \mathbf{1}_2 - \Phi_2 \Phi_2^\dagger) - \tfrac{1}{2} \delta_{ij} g^2 (\Phi_1 \Phi_1^\dagger - \Phi_2 \Phi_2^\dagger) \\
&\quad + \delta_{ij} (\tfrac{1}{4} g^2 - \tfrac{1}{12} g'^2) (\Phi_1^\dagger \Phi_1 - \Phi_2^\dagger \Phi_2) \mathbf{1}_2, \\
(\tilde{\mathbf{M}}^2)_{\tilde{U}_i^\dagger \tilde{Q}_j} &= (\tilde{\mathbf{M}}^2)^\dagger_{\tilde{Q}_j^\dagger \tilde{U}_i} = -(\mathbf{a}_u)_{ij} \Phi_2^T i\tau_2 + (\mathbf{h}_u)_{ij} \mu^* \Phi_1^T i\tau_2, \\
(\tilde{\mathbf{M}}^2)_{\tilde{D}_i^\dagger \tilde{Q}_j} &= (\tilde{\mathbf{M}}^2)^\dagger_{\tilde{Q}_j^\dagger \tilde{D}_i} = (\mathbf{a}_d)_{ij} \Phi_1^\dagger - (\mathbf{h}_d)_{ij} \mu^* \Phi_2^\dagger, \\
(\tilde{\mathbf{M}}^2)_{\tilde{U}_i^\dagger \tilde{U}_j} &= (\tilde{\mathbf{M}}_U^2)_{ij} + (\mathbf{h}_u \mathbf{h}_u^\dagger)_{ij} \Phi_2^\dagger \Phi_2 + \tfrac{1}{3} \delta_{ij} g'^2 (\Phi_1^\dagger \Phi_1 - \Phi_2^\dagger \Phi_2), \\
(\tilde{\mathbf{M}}^2)_{\tilde{D}_i^\dagger \tilde{D}_j} &= (\tilde{\mathbf{M}}_D^2)_{ij} + (\mathbf{h}_d \mathbf{h}_d^\dagger)_{ij} \Phi_1^\dagger \Phi_1 - \tfrac{1}{6} \delta_{ij} g'^2 (\Phi_1^\dagger \Phi_1 - \Phi_2^\dagger \Phi_2), \\
(\tilde{\mathbf{M}}^2)_{\tilde{U}_i^\dagger \tilde{D}_j} &= (\tilde{\mathbf{M}}^2)^\dagger_{\tilde{D}_j^\dagger \tilde{U}_i} = (\mathbf{h}_u \mathbf{h}_d^\dagger)_{ij} \Phi_1^T i\tau_2 \Phi_2,
\end{aligned} \tag{3.5}$$

where δ_{ij} is the usual Kronecker symbol.

The form of the derived effective Lagrangian depends, to some extent, on the choice of renormalization scheme. As usual, one may adopt the $\overline{\text{MS}}$ or $\overline{\text{DR}}$ schemes of renormalization. In general, the different schemes affect the holomorphic part of the Lagrangian at the one-loop level. Thanks to the nonrenormalization theorems of SUSY, the Yukawa couplings $\mathbf{h}_{u,d}$ are not renormalized, and the wave functions of $\Phi_{1,2}$, Q_{iL}, u_{iR}, and d_{iR} remove the ultraviolet (UV) divergences of the one-loop corrections to the Yukawa couplings $\bar{d}_{iR} \Phi_1^\dagger Q_{jL}$ and $\bar{u}_{iR} \Phi_2 Q_{jL}$. The leftover UV-finite terms are not $\tan\beta$ enhanced and can be absorbed into the definition of $\mathbf{h}_{u,d}$, up to higher-order scheme-dependent corrections. Although the latter could be consistently included in our gauge-symmetric and flavor-covariant formalism, we ignore these small UV-finite holomorphic terms as they are higher-order effects beyond the one-loop approximation of our interest.

By analogy, the gauge- and flavor-covariant effective Lagrangian for the up-type quark self-energies may be written down as follows:

$$\begin{aligned}
-\mathcal{L}^u_{\text{eff}}[\Phi_1, \Phi_2] &= \bar{u}^0_{iR} (\mathbf{h}_u \Phi_2^T (-i\tau_2) \\
&\quad + \Delta \mathbf{h}_u[\Phi_1, \Phi_2])_{ij} Q^0_{jL} + \text{H.c.},
\end{aligned} \tag{3.6}$$

where $\Delta \mathbf{h}_u[\Phi_1, \Phi_2]$ may be calculated from Feynman diagrams analogous to Fig. 1. As opposed to the down-type quark self-energy case, these radiative corrections are not enhanced for large values of $\tan\beta$ and so are ignored in our numerical analysis in Sec. V.

The weak quark chiral states, $u^0_{L,R}$ and $d^0_{L,R}$, are related to their respective mass eigenstates, $u_{L,R}$ and $d_{L,R}$, through the unitary transformations:

$$\begin{aligned}
u^0_L &= \mathbf{U}^Q_L u_L, \qquad & d^0_L &= \mathbf{U}^Q_L \mathbf{V} d_L, \\
u^0_R &= \mathbf{U}^u_R u_R, \qquad & d^0_R &= \mathbf{U}^d_R d_R,
\end{aligned} \tag{3.7}$$

where $\mathbf{U}^Q_L$, $\mathbf{U}^{u,d}_R$ are 3×3 unitary matrices and $\mathbf{V}$ is the CKM mixing matrix. All these unitary matrices are determined by the simple mass renormalization conditions:

$$\begin{aligned}
\langle \mathcal{L}^d_{\text{eff}}[\Phi_1, \Phi_2] \rangle &= -\bar{d}_R \hat{\mathbf{M}}_d d_L + \text{H.c.}, \\
\langle \mathcal{L}^u_{\text{eff}}[\Phi_1, \Phi_2] \rangle &= -\bar{u}_R \hat{\mathbf{M}}_u u_L + \text{H.c.},
\end{aligned} \tag{3.8}$$

where $\langle \ldots \rangle$ denotes the value when the Higgs doublets $\Phi_{1,2}$ acquire their VEVs, and $\hat{\mathbf{M}}_{u,d}$ are the physical diagonal mass matrices for the up- and down-type quarks. Imposing the conditions (3.8) yields [12]

$$\begin{aligned}
\mathbf{U}^{d\dagger}_R \mathbf{h}_d \mathbf{U}^Q_L &= \frac{\sqrt{2}}{v_1} \hat{\mathbf{M}}_d \mathbf{V}^\dagger \mathbf{R}_d^{-1}, \\
\mathbf{U}^{u\dagger}_R \mathbf{h}_u \mathbf{U}^Q_L &= \frac{\sqrt{2}}{v_2} \hat{\mathbf{M}}_u \mathbf{R}_u^{-1},
\end{aligned} \tag{3.9}$$

where

$$\begin{aligned}
\mathbf{R}_d &= \mathbf{1} + \frac{\sqrt{2}}{v_1} \mathbf{U}^{Q\dagger}_L \langle \mathbf{h}_d^{-1} \Delta \mathbf{h}_d[\Phi_1, \Phi_2] \rangle \mathbf{U}^Q_L, \\
\mathbf{R}_u &= \mathbf{1} + \frac{\sqrt{2}}{v_2} \mathbf{U}^{Q\dagger}_L \langle \mathbf{h}_u^{-1} \Delta \mathbf{h}_u[\Phi_1, \Phi_2] \rangle \mathbf{U}^Q_L.
\end{aligned} \tag{3.10}$$

In (3.10) and in the following, the symbol $\mathbf{1}$ without a subscript will always denote the 3×3 unit matrix. We observe that the unitary matrices $\mathbf{U}^Q_L$, $\mathbf{U}^{u,d}_R$ can all be set to $\mathbf{1}$ by virtue of the flavor transformations given in (2.4). The Yukawa couplings $\mathbf{h}_{u,d}$ are determined by the physical mass conditions (3.9). It is important to remark here [12] that these conditions form a coupled system of nonlinear

equations with respect to $\mathbf{h}_{u,d}$, since the Yukawa couplings also enter the right sides of (3.9) through the expressions $\mathbf{R}_{d,u}$ in (3.10). In addition, one should notice that the physical CKM mixing matrix $\mathbf{V}$ remains unitary throughout our effective Lagrangian approach. As we will see below and more explicitly in Appendix B, the unitarity of $\mathbf{V}$ throughout the renormalization process is a crucial property for maintaining the gauge symmetries through the Ward identities (WIs) in our effective Lagrangian formalism.

We now consider the effective FCNC Lagrangian related to Higgs interactions to down-type quarks. From (3.1), we find that

$$\begin{aligned}-\mathcal{L}_{\rm eff}^{d,H} &= \bar{d}_R \frac{\mathbf{h}_d}{\sqrt{2}}[\phi_1(\mathbf{1}+\mathbf{\Delta}_d^{\phi_1}) - ia_1(\mathbf{1}+\mathbf{\Delta}_d^{a_1}) \\ &\quad + \phi_2 \mathbf{\Delta}_d^{\phi_2} - ia_2 \mathbf{\Delta}_d^{a_2}]\mathbf{V} d_L \\ &\quad + \bar{d}_R \mathbf{h}_d[\phi_1^-(\mathbf{1}+\mathbf{\Delta}_d^{\phi_1^-}) + \phi_2^- \mathbf{\Delta}_d^{\phi_2^-}]u_L + \text{H.c.},\end{aligned} \tag{3.11}$$

where the individual components of the Higgs doublets $\Phi_{1,2}$ are given by

$$\Phi_{1,2} = \begin{pmatrix} \phi_{1,2}^+ \\ \frac{1}{\sqrt{2}}(v_{1,2} + \phi_{1,2} + ia_{1,2}) \end{pmatrix}. \tag{3.12}$$

Moreover, the 3×3 matrices $\mathbf{\Delta}_d^{\phi_{1,2}}$, $\mathbf{\Delta}_d^{a_{1,2}}$, and $\mathbf{\Delta}_d^{\phi_{1,2}^\pm}$ are given by

$$\begin{aligned}\mathbf{\Delta}_d^{\phi_{1,2}} &= \sqrt{2}\left\langle \frac{\delta}{\delta \phi_{1,2}} \mathbf{\Delta}_d \right\rangle, \qquad \mathbf{\Delta}_d^{a_{1,2}} = i\sqrt{2}\left\langle \frac{\delta}{\delta a_{1,2}} \mathbf{\Delta}_d \right\rangle, \\ \mathbf{\Delta}_d^{\phi_{1,2}^\pm} &= \left\langle \frac{\delta}{\delta \phi_{1,2}^\pm} \mathbf{\Delta}_d \right\rangle,\end{aligned} \tag{3.13}$$

where we have used the short-hand notation, $\mathbf{\Delta}_d \equiv \mathbf{h}_d^{-1}\Delta\mathbf{h}_d[\Phi_1, \Phi_2]$, and suppressed the vanishing isodoublet components on the LHS's of (3.13). In the CP-violating MSSM, the weak-state Higgs fields $\phi_{1,2}$, $a_{1,2}$, and $\phi_{1,2}^-$ are related to the neutral CP-mixed mass eigenstates $H_{1,2,3}$ [21,23], the charged-Higgs boson H^-, and the would-be Goldstone bosons G^0 and G^-, associated with the Z and W^- bosons, through:

$$\begin{aligned}\phi_1 &= O_{1i}H_i, & \phi_2 &= O_{2i}H_i, \\ a_1 &= c_\beta G^0 - s_\beta O_{3i}H_i, & a_2 &= s_\beta G^0 + c_\beta O_{3i}H_i, \\ \phi_1^- &= c_\beta G^- - s_\beta H^-, & \phi_2^- &= s_\beta G^- + c_\beta H^-,\end{aligned} \tag{3.14}$$

where $s_\beta \equiv \sin\beta$, $c_\beta \equiv \cos\beta$ and O is an orthogonal 3×3 Higgs-boson-mixing matrix.

One may now exploit the properties of gauge and flavor covariance of the effective functional $\mathbf{\Delta}_d[\Phi_1, \Phi_2]$ to obtain useful relations in the large-$\tan\beta$ limit. Specifically, $\mathbf{\Delta}_d[\Phi_1, \Phi_2]$ should have the form:

$$\mathbf{\Delta}_d[\Phi_1, \Phi_2] = \Phi_1^\dagger \mathbf{f}_1 + \Phi_2^\dagger \mathbf{f}_2, \tag{3.15}$$

where $\mathbf{f}_{1,2}(\Phi_1^\dagger\Phi_1, \Phi_2^\dagger\Phi_2, \Phi_1^\dagger\Phi_2, \Phi_2^\dagger\Phi_1)$ are calculable 3×3-dimensional functionals which transform as $\mathbf{h}_d^\dagger \mathbf{h}_d$ or $\mathbf{h}_u^\dagger \mathbf{h}_u$ under the flavor rotations (2.4). Given the form (3.15), it is then not difficult to show that in the infinite-$\tan\beta$ limit ($v_1 \to 0$),

$$\begin{aligned}\lim_{v_1\to 0} i\sqrt{2}\left\langle \frac{\delta}{\delta a_2} \mathbf{\Delta}_d \right\rangle &= \frac{\sqrt{2}}{v_2}\langle \mathbf{\Delta}_d \rangle, \\ \lim_{v_1\to 0} \left\langle \frac{\delta}{\delta \phi_2^-} \mathbf{\Delta}_d \right\rangle &= \frac{\sqrt{2}}{v_2}\langle \mathbf{\Delta}_d \rangle.\end{aligned} \tag{3.16}$$

Very similar relations may be derived for the up-type quark sector, but in the limit of vanishing $\tan\beta$. As we show in Appendix B, Ward identities (WIs) involving the W^- and Z-boson couplings to quarks give rise to the following *exact* relations:

$$\begin{aligned}\mathbf{\Delta}_d^{G^0} &\equiv i\sqrt{2}\left\langle \frac{\delta}{\delta G^0} \mathbf{\Delta}_d \right\rangle = \frac{\sqrt{2}}{v}\langle \mathbf{\Delta}_d \rangle, \\ \mathbf{\Delta}_d^{G^-} &\equiv \left\langle \frac{\delta}{\delta G^-} \mathbf{\Delta}_d \right\rangle = \frac{\sqrt{2}}{v}\langle \mathbf{\Delta}_d \rangle,\end{aligned} \tag{3.17}$$

where $v = \sqrt{v_1^2 + v_2^2}$ is the VEV of the Higgs boson in the SM. Relations very analogous to those stated in (3.17) hold true for the up-type sector as well, i.e. $\mathbf{\Delta}_u^{G^0} = \mathbf{\Delta}_u^{G^+} = -\sqrt{2}\langle \mathbf{\Delta}_u \rangle / v$, where the extra minus sign comes from the opposite isospin of the up-type quarks with respect to the down-type quarks.

For our phenomenological analysis in Sec. IV, we may conveniently express the general flavor-changing (FC) effective Lagrangian for the interactions of the neutral and charged-Higgs fields to the up- and down-type quarks u, d in the following form:

$$\begin{aligned}\mathcal{L}_{\rm FC} &= -\frac{g}{2M_W}[H_i \bar{d}(\hat{\mathbf{M}}_d \mathbf{g}_{H_i\bar{d}d}^L P_L + \mathbf{g}_{H_i\bar{d}d}^R \hat{\mathbf{M}}_d P_R)d \\ &\quad + G^0 \bar{d}\hat{\mathbf{M}}_d i\gamma_5 d + H_i \bar{u}(\hat{\mathbf{M}}_u \mathbf{g}_{H_i\bar{u}u}^L P_L \\ &\quad + \mathbf{g}_{H_i\bar{u}u}^R \hat{\mathbf{M}}_u P_R)u - G^0 \bar{u}\hat{\mathbf{M}}_u i\gamma_5 u] \\ &\quad - \frac{g}{\sqrt{2}M_W}[H^- \bar{d}(\hat{\mathbf{M}}_d \mathbf{g}_{H^-\bar{d}u}^L P_L + \mathbf{g}_{H^-\bar{d}u}^R \hat{\mathbf{M}}_u P_R)u \\ &\quad + G^- \bar{d}(\hat{\mathbf{M}}_d \mathbf{V}^\dagger P_L - \mathbf{V}^\dagger \hat{\mathbf{M}}_u P_R)u + \text{H.c.}],\end{aligned} \tag{3.18}$$

where the Higgs couplings in the flavor basis $\mathbf{U}_L^Q = \mathbf{U}_R^u = \mathbf{U}_R^d = \mathbf{1}$ are given by

$$\begin{aligned}\mathbf{g}_{H_i\bar{d}d}^L &= \frac{O_{1i}}{c_\beta}\mathbf{V}^\dagger \mathbf{R}_d^{-1}(\mathbf{1}+\mathbf{\Delta}_d^{\phi_1})\mathbf{V} + \frac{O_{2i}}{c_\beta}\mathbf{V}^\dagger \mathbf{R}_d^{-1}\mathbf{\Delta}_d^{\phi_2}\mathbf{V} \\ &\quad + iO_{3i}t_\beta \mathbf{V}^\dagger \mathbf{R}_d^{-1}\left(\mathbf{1} + \mathbf{\Delta}_d^{a_1} - \frac{1}{t_\beta}\mathbf{\Delta}_d^{a_2}\right)\mathbf{V},\end{aligned} \tag{3.19}$$

$$\mathbf{g}_{H_i\bar{d}d}^R = (\mathbf{g}_{H_i\bar{d}d}^L)^\dagger, \tag{3.20}$$

$$\mathbf{g}^{L}_{H_i\bar{u}u} = \frac{O_{1i}}{s_\beta}\mathbf{R}_u^{-1}\mathbf{\Delta}_u^{\phi_1} + \frac{O_{2i}}{s_\beta}\mathbf{R}_u^{-1}(\mathbf{1} + \mathbf{\Delta}_u^{\phi_2}) + iO_{3i}t_\beta^{-1}\mathbf{R}_u^{-1}(\mathbf{1} - \mathbf{\Delta}_u^{a_2} + t_\beta\mathbf{\Delta}_u^{a_1}), \quad (3.21)$$

$$\mathbf{g}^{R}_{H_i\bar{u}u} = (\mathbf{g}^{L}_{H_i\bar{u}u})^\dagger, \quad (3.22)$$

$$\mathbf{g}^{L}_{H^-\bar{d}u} = -t_\beta\mathbf{V}^\dagger\mathbf{R}_d^{-1}(\mathbf{1} + \mathbf{\Delta}_d^{\phi_1^-}) + \mathbf{V}^\dagger\mathbf{R}_d^{-1}\mathbf{\Delta}_d^{\phi_2^-}, \quad (3.23)$$

$$\mathbf{g}^{R}_{H^-\bar{d}u} = -t_\beta^{-1}\mathbf{V}^\dagger(\mathbf{1} - (\mathbf{\Delta}_u^{\phi_2^+})^\dagger)(\mathbf{R}_u^{-1})^\dagger - \mathbf{V}^\dagger(\mathbf{\Delta}_u^{\phi_1^+})^\dagger(\mathbf{R}_u^{-1})^\dagger, \quad (3.24)$$

and $t_\beta \equiv \tan\beta$. We note that the Higgs-boson vertex-correction matrices for the up-type quarks, $\mathbf{\Delta}_u^{\phi_{1,2}}$, $\mathbf{\Delta}_u^{a_{1,2}}$, and $\mathbf{\Delta}_u^{\phi^\pm_{1,2}}$, are defined as in (3.13).

The above general form of the effective Lagrangian $\mathcal{L}_{\rm FC}$ extends the one derived in [12] in several aspects. First, it consistently includes all higher-order terms of the form $(t_\beta m_b\mu/M^2_{\rm SUSY})^{n\geq 1}$, which can become important in scenarios with large bottom-squark mixing [5]. Second, it does not suffer from the limitation that the soft SUSY-breaking scale should be much higher than the electroweak scale M_Z. Specifically, SM electroweak corrections may be included in the Coleman-Weinberg-type effective functionals $\mathbf{\Delta}_{d,u}[\Phi_1, \Phi_2]$, provided the theory is quantized in nonlinear gauges [24] that preserve the Higgs-boson low-energy theorem (HLET) [25]. Finally, the effective Lagrangian $\mathcal{L}_{\rm FC}$ implements properly all the gauge symmetries through the WIs as discussed in Appendix B.

The general FC effective Lagrangian (3.18) takes on the form presented in [12] in the single-Higgs-insertion approximation. In this case, the $\tan\beta$-enhanced threshold corrections $\mathbf{\Delta}_d^{a_2}$, $\mathbf{\Delta}_d^{\phi_2}$, $\mathbf{\Delta}_d^{\phi_2^\pm}$, and $\langle\mathbf{\Delta}_d\rangle$ are interrelated as follows:

$$\frac{\sqrt{2}}{v_2}\langle\mathbf{\Delta}_d\rangle = \mathbf{\Delta}_d^{a_2} = \mathbf{\Delta}_d^{\phi_2} = \mathbf{\Delta}_d^{\phi_2^-} = (\mathbf{\Delta}_d^{\phi_2^+})^\dagger, \quad (3.25)$$

where $\langle\mathbf{\Delta}_d\rangle$ is given in the MSSM with MCPMFV by

$$\frac{\sqrt{2}}{v_2}\langle\mathbf{\Delta}_d\rangle = \mathbf{1}\frac{2\alpha_3}{3\pi}\mu^* M_3^* I(\tilde{M}_Q^2, \tilde{M}_D^2, |M_3|^2) + \frac{\mathbf{h}_u^\dagger\mathbf{h}_u}{16\pi^2}\mu^* A_u I(\tilde{M}_Q^2, \tilde{M}_U^2, |\mu|^2) + \ldots, \quad (3.26)$$

and $I(x, y, z)$ is the one-loop function:

$$I(x, y, z) = \frac{xy\ln(x/y) + yz\ln(y/z) + xz\ln(z/x)}{(x-y)(y-z)(x-z)}. \quad (3.27)$$

The ellipses in (3.26) denote the small contributions coming from the Feynman diagram in Fig. 1(c), which has the same flavor structure as the gluino-mediated graph in Fig. 1(a), i.e., this contribution is flavor-singlet in the single-Higgs-insertion approximation. We remark, finally, that in writing down (3.26) we have not considered the RG-running effects on the squark mass matrices between $M_{\rm GUT}$ and $M_{\rm SUSY}$. These effects are important, and are taken into account in our numerical analysis in Sec. V.

In addition to graphs involving SUSY particles, the two-Higgs-doublet model (2HDM) sector of the MSSM may also contribute significantly to the one-loop self-energy graphs of the down quarks. This contribution is shown in Fig. 2 and is formally enhanced at large $\tan\beta$, since it is proportional to $\mathbf{h}_d$. In the single-Higgs-insertion approximation, the 2HDM contribution is given by

$$\frac{\sqrt{2}}{v_2}\langle\mathbf{\Delta}_d^{\rm 2HDM}\rangle = \frac{\mathbf{h}_u^\dagger\mathbf{h}_u}{16\pi^2}\frac{B^*\mu^*}{M^2_{H_d} - M^2_{H_u}}\ln\left|\frac{M^2_{H_d} + |\mu|^2}{M^2_{H_u} + |\mu|^2}\right|. \quad (3.28)$$

This contribution turns out to be subleading with respect to the Feynman diagram 1(b) and exhibits a very similar flavor structure. Beyond the single-Higgs-insertion approximation, the effective functional $\Delta\mathbf{h}_d^{\rm 2HDM}[\Phi_1, \Phi_2]$ is calculated as

$$(\Delta\mathbf{h}_d^{\rm 2HDM})_{ij} = \int\frac{d^nk}{(2\pi)^n i}(\mathbf{h}_d)_{il}P_L \times\left(\frac{1}{\not{k}\mathbf{1}_6 - \mathbf{M}_q P_L - \mathbf{M}_q^\dagger P_R}\right)_{Q_l\bar{u}_k} P_L(\mathbf{h}_u)_{kj} \times\left(\frac{1}{k^2\mathbf{1}_4 - \mathbf{M}_H^2}\right)_{\Phi_1\Phi_2^\dagger}, \quad (3.29)$$

where $\mathbf{M}_q[\Phi_1, \Phi_2]$ and $\mathbf{M}_H^2[\Phi_1, \Phi_2]$ are the 6×6- and 4×4-dimensional quark and Higgs-boson mass matrices in the background of nonzero $\Phi_{1,2}$. The 6×6-dimensional quark mass matrix is given by

$$\mathbf{M}_q[\Phi_1, \Phi_2] = \begin{pmatrix}(\mathbf{M}_q)_{\bar{u}_i Q_j}\\ (\mathbf{M}_q)_{\bar{d}_i Q_j}\end{pmatrix} = \begin{pmatrix}(\mathbf{h}_u)_{ij}\Phi_2^T(-i\tau_2)\\ (\mathbf{h}_d)_{ij}\Phi_1^\dagger\end{pmatrix}. \quad (3.30)$$

The Higgs-boson background mass matrix $\mathbf{M}_H^2[\Phi_1, \Phi_2]$ receives appreciable radiative corrections beyond the tree level [19,21,23,26]. At the tree level, the 4×4-dimensional matrix $\mathbf{M}_H^2[\Phi_1, \Phi_2]$ is given in the weak basis (Φ_1, Φ_2) by

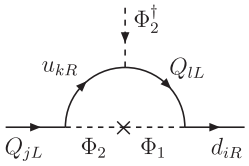

FIG. 2. Two-Higgs-doublet model (2HDM) contribution to the one-loop self-energy graphs for down-type quarks in the single-Higgs-insertion approximation.

$$\mathbf{M}_H^2[\Phi_1,\Phi_2]=\begin{pmatrix}(\mathbf{M}_H^2)_{\Phi_1^\dagger\Phi_1} & (\mathbf{M}_H^2)_{\Phi_1^\dagger\Phi_2}\\ (\mathbf{M}_H^2)_{\Phi_2^\dagger\Phi_1} & (\mathbf{M}_H^2)_{\Phi_2^\dagger\Phi_2}\end{pmatrix}, \tag{3.31}$$

where

$$\begin{aligned}(\mathbf{M}_H^2)_{\Phi_1^\dagger\Phi_1}&=\Big(M_{H_d}^2+|\mu|^2+\frac{g^2+g'^2}{2}\Phi_1^\dagger\Phi_1\\&\quad+\frac{g^2-g'^2}{4}\Phi_2^\dagger\Phi_2\Big)\mathbf{1}_2+\frac{g^2}{2}\Phi_2\Phi_2^\dagger,\\(\mathbf{M}_H^2)_{\Phi_2^\dagger\Phi_2}&=\Big(M_{H_u}^2+|\mu|^2+\frac{g^2+g'^2}{2}\Phi_2^\dagger\Phi_2\\&\quad+\frac{g^2-g'^2}{4}\Phi_1^\dagger\Phi_1\Big)\mathbf{1}_2+\frac{g^2}{2}\Phi_1\Phi_1^\dagger,\\(\mathbf{M}_H^2)_{\Phi_1^\dagger\Phi_2}&=(\mathbf{M}_H^2)^\dagger_{\Phi_2^\dagger\Phi_1}=\Big(-B\mu+\frac{g^2}{2}\Phi_2^\dagger\Phi_1\Big)\mathbf{1}_2\\&\quad+\frac{g^2-g'^2}{4}\Phi_1\Phi_2^\dagger.\end{aligned} \tag{3.32}$$

In the one-loop effective Lagrangian $\mathcal{L}_{\rm FC}$ given in (3.18), the couplings of the Goldstone bosons G^0 and $G^\pm$ to quarks retain their tree-level form. This result is not accidental, but a consequence of the Goldstone theorem, which applies when the momenta of the external particles are all set to zero. However, the tree-level form of the Goldstone couplings gets modified when momentum-dependent (derivative) terms are considered. To leading order in a derivative expansion, one would have to consider the effective Lagrangian

$$\begin{aligned}\mathcal{L}_{\not p}&=i\bar{Q}_L[\mathbf{Z}_Q\not p+\mathbf{A}_Q^{(i,j)}(\Phi_i^\dagger(\not p\Phi_j)-(\not p\Phi_j)^\dagger\Phi_i)\\&\quad+\mathbf{B}_Q^{(i,j)}(\Phi_i(\not p\Phi_j)^\dagger-(\not p\Phi_j)\Phi_i^\dagger)]Q_L+\ldots,\end{aligned} \tag{3.33}$$

where the dots denote analogous terms for the right-handed up- and down-type quarks u_R and d_R. The first term depending on $\mathbf{Z}_Q$ is a functional of $\Phi_{1,2}$ for the left-handed quarks Q_L. Such a term is not $\tan\beta$ enhanced and renormalization-scheme dependent. As mentioned above, these terms can be neglected to a good approximation. The effective functionals $\mathbf{A}_Q^{(i,j)}[\Phi_1,\Phi_2]$ and $\mathbf{B}_Q^{(i,j)}[\Phi_1,\Phi_2]$ are UV finite and include large Yukawa-coupling effects due to h_t.[2] In particular, this is the case for the effective functionals with $i=j=2$. One typical graph of such a contribution is displayed in Fig. 3. Because of gauge invariance, analogous contributions will be present in the one-loop Z- and W-boson couplings. All these effects are not enhanced by $\tan\beta$, and can be consistently neglected without spoiling the gauge symmetries of the effective Lagrangian $\mathcal{L}_{\rm FC}$.

[2]These effects have first been identified and studied in [27] within the standard model.

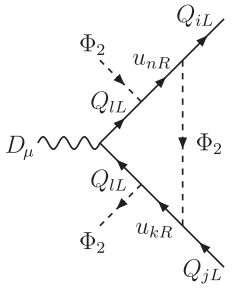

FIG. 3. Dominant gauge- and flavor-invariant contribution leading to a modification of the tree-level Goldstone-boson couplings to quarks.

In the next two sections, we present analytic and numerical results related to FCNC B-meson observables, using the effective Lagrangian (3.18) and including the 2HDM contribution (3.29).

IV. FCNC B-MESON OBSERVABLES

In this section, our interest will be in FCNC B-meson observables, such as the $B_{d,s}^0$-$\bar{B}_{d,s}^0$ mass differences $\Delta M_{B_{d,s}}$, and the decays $B_{s,d}\to\mu^+\mu^-$, $B_u\to\tau\nu$, and $B\to X_s\gamma$.

A. $\Delta M_{B_{d,s}}$

Our discussion and conventions here follow closely [12]. In the approximation of equal B-meson lifetimes, the SM and SUSY contributions to $\Delta M_{B_{d,s}}$ may be written separately, as follows:

$$\Delta M_{B_q}=2|\langle\bar{B}_q^0|H_{\rm eff}^{\Delta B=2}|B_q^0\rangle_{\rm SM}+\langle\bar{B}_q^0|H_{\rm eff}^{\Delta B=2}|B_q^0\rangle_{\rm SUSY}|, \tag{4.1}$$

where $q\equiv d,s$ and $H_{\rm eff}^{\Delta B=2}$ is the effective $\Delta B=2$ Hamiltonian. Neglecting the subdominant SM contribution, the SUSY contributions to the $\Delta B=2$ transition amplitudes are given by

$$\begin{aligned}\langle\bar{B}_d^0|H_{\rm eff}^{\Delta B=2}|B_d^0\rangle_{\rm SUSY}&=1711\ {\rm ps}^{-1}\Big(\frac{\hat{B}_{B_d}^{1/2}F_{B_d}}{230\ {\rm MeV}}\Big)^2\Big(\frac{\eta_B}{0.55}\Big)\\&\quad\times[0.88(C_2^{\rm LR(DP)}+C_2^{\rm LR(2HDM)})\\&\quad-0.52(C_1^{\rm SLL(DP)}+C_1^{\rm SRR(DP)})],\\\langle\bar{B}_s^0|H_{\rm eff}^{\Delta B=2}|B_s^0\rangle_{\rm SUSY}&=2310\ {\rm ps}^{-1}\Big(\frac{\hat{B}_{B_s}^{1/2}F_{B_s}}{265\ {\rm MeV}}\Big)^2\Big(\frac{\eta_B}{0.55}\Big)\\&\quad\times[0.88(C_2^{\rm LR(DP)}+C_2^{\rm LR(2HDM)})\\&\quad-0.52(C_1^{\rm SLL(DP)}+C_1^{\rm SRR(DP)})\Big],\end{aligned} \tag{4.2}$$

where DP stands for the Higgs-mediated double-penguin effect. In addition, we have used the next-to-leading order QCD factors determined in [28–32], along with their

hadronic matrix elements at the scale $\mu = 4.2$ GeV:

$$\bar{P}_1^{\rm LR} = -0.58, \qquad \bar{P}_2^{\rm LR} = 0.88, \\ \bar{P}_1^{\rm SLL} = -0.52, \qquad \bar{P}_2^{\rm SLL} = -1.1. \tag{4.3}$$

The Wilson coefficients occurring in (4.2) are given by

$$C_1^{\rm SLL(DP)} = -\frac{16\pi^2 m_b^2}{\sqrt{2}G_F M_W^2}\sum_{i=1}^{3}\frac{\mathbf{g}^L_{H_i\bar{b}q}\mathbf{g}^L_{H_i\bar{b}q}}{M^2_{H_i}}, \\ C_1^{\rm SRR(DP)} = -\frac{16\pi^2 m_q^2}{\sqrt{2}G_F M_W^2}\sum_{i=1}^{3}\frac{\mathbf{g}^R_{H_i\bar{b}q}\mathbf{g}^R_{H_i\bar{b}q}}{M^2_{H_i}}, \\ C_2^{\rm LR(DP)} = -\frac{32\pi^2 m_b m_q}{\sqrt{2}G_F M_W^2}\sum_{i=1}^{3}\frac{\mathbf{g}^L_{H_i\bar{b}q}\mathbf{g}^R_{H_i\bar{b}q}}{M^2_{H_i}}, \tag{4.4}$$

where the $\tan^2\beta$-enhanced couplings $\mathbf{g}^{L,R}_{H_i\bar{s}d}$ may be obtained from (3.18). Hence, the DP Wilson coefficients in (4.4) have a $\tan^4\beta$ dependence and, although two-loop suppressed, they become significant for large values of $\tan\beta \gtrsim 40$.

There are two relevant one-loop contributions to $\langle\bar{B}^0|H_{\rm eff}^{\Delta B=2}|B^0\rangle_{\rm SUSY}$ at large $\tan\beta$: (i) the t-$H^\pm$ box contribution to $C_2^{\rm LR}$ of the 2HDM type, and (ii) the one-loop chargino-stop box diagram contributing to $C_1^{\rm SLL}$. To a good approximation, $C_2^{\rm LR(2HDM)}$ may be given by [32]

$$C_2^{\rm LR(2HDM)} \approx -\frac{2m_b m_q}{M_W^2}(V_{tb}^* V_{tq})^2\tan^2\beta. \tag{4.5}$$

In the kinematic region $M_{H^\pm} \approx m_t$, the above contribution can amount to as much as 10% of the DP effects mentioned above. This estimate is obtained by noticing that the light-quark masses in (4.4) and (4.5) are running and are evaluated at the top-quark mass scale, i.e., $m_s(m_t) \simeq 90$ MeV, $m_d(m_t) \simeq 4$ MeV [33]. The second contribution (ii) turns out to be non-negligible only for small values of the μ-parameter [32], i.e., for $|\mu| \lesssim 200$ GeV.

B. $\bar{B}^0_{d,s} \to \mu^+\mu^-$

The leptonic decays of neutral B mesons, $\bar{B}^0_{d,s} \to \mu^+\mu^-$, are enhanced at large values of $\tan\beta$ [6–15]. Neglecting contributions proportional to the lighter quark masses $m_{d,s}$, the relevant effective Hamiltonian for $\Delta B = 1$ FCNC transitions is given by

$$H_{\rm eff}^{\Delta B=1} = -2\sqrt{2}G_F V_{tb}V_{tq}^*(C_S\mathcal{O}_S + C_P\mathcal{O}_P + C_{10}\mathcal{O}_{10}), \tag{4.6}$$

where

$$\mathcal{O}_S = \frac{e^2}{16\pi^2}m_b(\bar{q}P_R b)(\bar{\mu}\mu), \\ \mathcal{O}_P = \frac{e^2}{16\pi^2}m_b(\bar{q}P_R b)(\bar{\mu}\gamma_5\mu), \\ \mathcal{O}_{10} = \frac{e^2}{16\pi^2}(\bar{q}\gamma^\mu P_L b)(\bar{\mu}\gamma_\mu\gamma_5\mu). \tag{4.7}$$

Using the resummed FCNC effective Lagrangian (3.18), the Wilson coefficients C_S and C_P in the region of large values of $\tan\beta$ are given by

$$C_S = \frac{2\pi m_\mu}{\alpha_{\rm em}}\frac{1}{V_{tb}V_{tq}^*}\sum_{i=1}^{3}\frac{\mathbf{g}^R_{H_i\bar{q}b}g^S_{H_i\bar{\mu}\mu}}{M^2_{H_i}}, \\ C_P = i\frac{2\pi m_\mu}{\alpha_{\rm em}}\frac{1}{V_{tb}V_{tq}^*}\sum_{i=1}^{3}\frac{\mathbf{g}^R_{H_i\bar{q}b}g^P_{H_i\bar{\mu}\mu}}{M^2_{H_i}}, \tag{4.8}$$

where $C_{10} = -4.221$ denotes the leading SM contribution. In addition, the reduced scalar and pseudoscalar Higgs couplings to charged leptons $g^{S,P}_{H_i\bar{\mu}\mu}$ in (4.8) are given by

$$g^S_{H_i\bar{\mu}\mu} = \frac{O_{1i}}{\cos\beta}, \qquad g^P_{H_i\bar{\mu}\mu} = -\tan\beta O_{3i}. \tag{4.9}$$

Here we neglect the nonholomorphic vertex effects on the leptonic sector since they are unobservably small.

Taking into consideration the aforementioned approximations, the branching ratio for $\bar{B}^0_{d,s} \to \mu^+\mu^-$ is found to be [8]

$$B(\bar{B}^0_q \to \mu^+\mu^-) = \frac{G_F^2\alpha_{\rm em}^2}{16\pi^3}M_{B_q}\tau_{B_q}|V_{tb}V_{tq}^*|^2 \\ \times\sqrt{1-\frac{4m_\mu^2}{M_{B_q}^2}}\left[\left(1-\frac{4m_\mu^2}{M_{B_q}^2}\right)|F_S^q|^2 \right. \\ \left. + |F_P^q + 2m_\mu F_A^q|^2\right], \tag{4.10}$$

where $q = d, s$ and τ_{B_q} is the total lifetime of the B_q meson. Moreover, the form factors $F^q_{S,P,A}$ are given by

$$F^q_{S,P} = -\frac{i}{2}M^2_{B_q}F_{B_q}\frac{m_b}{m_b+m_q}C_{S,P}, \\ F^q_A = -\frac{i}{2}F_{B_q}C_{10}. \tag{4.11}$$

Although the Wilson coefficient C_{10} is subdominant for $\tan\beta \gtrsim 40$, its effect has been included in our numerical estimates.

C. $B_u \to \tau\nu$

There is an important tree-level charged-Higgs-boson contribution to $B_u \to \tau\nu$ decay [16,17]. It is not helicity

suppressed and interferes destructively with the SM contribution [34]. The ratio of the branching ratio to the SM value is given by

$$R_{B\tau\nu} = \frac{B(B^- \to \tau^- \bar{\nu})}{B^{\rm SM}(B^- \to \tau^- \bar{\nu})} = \left| 1 + \tan\beta \frac{(\mathbf{g}^{L\dagger}_{H^-\bar{d}u})_{13}}{\mathbf{V}_{13}} \left(\frac{M_{B^\pm}}{M_{H^\pm}}\right)^2 \right|^2, \quad (4.12)$$

where $\mathbf{g}^L_{H^-\bar{d}u} = -\tan\beta \mathbf{V}^\dagger$ at tree level [cf. (3.23)], leading to the negative interference with the SM contribution.

D. $B \to X_s\gamma$

The relevant effective Hamiltonian for $B \to X_s\gamma$ is given by

$$H^{b\to s\gamma}_{\rm eff} = -\frac{4G_F}{\sqrt{2}} V_{tb}V^*_{ts} \Big\{ \sum_{i=2,7,8} C_i(\mu_b)\mathcal{O}_i(\mu_b) + C'_7(\mu_b)\mathcal{O}'_7(\mu_b) + C'_8(\mu_b)\mathcal{O}'_8(\mu_b) \Big\}, \quad (4.13)$$

with

$$\begin{aligned} \mathcal{O}_2 &= \bar{s}_L\gamma_\mu c_L \bar{c}_L \gamma^\mu b_L, \\ \mathcal{O}_7 &= \frac{em_b}{16\pi^2}\bar{s}_L\sigma_{\mu\nu}F^{\mu\nu}b_R; \\ \mathcal{O}'_7 &= \frac{em_b}{16\pi^2}\bar{s}_R\sigma_{\mu\nu}F^{\mu\nu}b_L, \\ \mathcal{O}_8 &= \frac{g_s m_b}{16\pi^2}\bar{s}_L\sigma_{\mu\nu}F^{\mu\nu}b_R; \\ \mathcal{O}'_8 &= \frac{g_s m_b}{16\pi^2}\bar{s}_R\sigma_{\mu\nu}F^{\mu\nu}b_L. \end{aligned} \quad (4.14)$$

We closely follow the calculations of Refs. [35] for the branching ratio $B(B \to X_s\gamma)$ and the direct CP asymmetry in the decay. For the running c quark mass, we use $m_c(m_c^{\rm pole})$ to capture a part of NNLO corrections [36]. We refer to, for example, Appendix B of Ref. [37] for the detailed expression of the branching ratio in terms of the Wilson coefficients which we are gong to present below.

The LO charged-Higgs contribution is given by

$$C^{(0)H^\pm}_{7,8}(M_W) = \frac{1}{3}\frac{(\mathbf{g}^{R\dagger}_{H^-\bar{d}u})_{33}}{\mathbf{V}_{33}}\frac{(\mathbf{g}^{R}_{H^-\bar{d}u})_{23}}{\mathbf{V}^\dagger_{23}}F^{(1)}_{7,8}(y) + \frac{(\mathbf{g}^{L\dagger}_{H^-\bar{d}u})_{33}}{\mathbf{V}_{33}}\frac{(\mathbf{g}^{R}_{H^-\bar{d}u})_{23}}{\mathbf{V}^\dagger_{23}}F^{(2)}_{7,8}(y), \quad (4.15)$$

where $y \equiv \bar{m}_t^2(M_W)/M^2_{H^\pm}$, the ratio of the top-quark running mass at the scale M_W to the charged-Higgs-boson pole mass. In the numerical analysis, we include the NLO contribution. Note that $\mathbf{g}^R_{H^-\bar{d}u} = -t_\beta^{-1}\mathbf{V}^\dagger$ and $\mathbf{g}^L_{H^-\bar{d}u} = -t_\beta\mathbf{V}^\dagger$ at tree level, see Eqs. (3.23) and (3.24). The functions $F^{(1),(2)}_{7,8}$ can be found in Refs. [37,38].

The chargino contributions are

$$\begin{aligned} C^{\chi^\pm}_{7,8}(\mu_{\rm SUSY}) = \sum_{i=1,2}\Big\{ &\frac{2}{3}\frac{M_W^2}{\tilde{m}_q^2}|(C_R)_{i1}|^2 F^{(1)}_{7,8}(x_{\tilde{q}\chi_i^-}) - \frac{(\mathbf{V}^\dagger\mathbf{R}_d^{-1})^\dagger_{13}\mathbf{V}^\dagger_{21} + (\mathbf{V}^\dagger\mathbf{R}_d^{-1})^\dagger_{23}\mathbf{V}^\dagger_{22}}{c_\beta\mathbf{V}_{33}\mathbf{V}^\dagger_{23}}\frac{(C_L)_{i2}(C_R)^*_{i1}M_W}{\sqrt{2}m_{\chi_i^-}}F^{(3)}_{7,8}(x_{\tilde{q}\chi_i^-}) \\ &- \frac{2}{3}\sum_{j=1,2}\left| (C_R)_{i1}(U^{\tilde{t}}_{1j})^* - \frac{(\hat{\mathbf{M}}_u\mathbf{R}_u^{-1})_{33}}{\sqrt{2}s_\beta M_W}(C_R)_{i2}(U^{\tilde{t}}_{2j})^* \right|^2 \frac{M_W^2}{m^2_{\tilde{t}_j}}F^{(1)}_{7,8}(x_{\tilde{t}_j\chi_i^-}) \\ &+ \frac{(\mathbf{V}^\dagger\mathbf{R}_d^{-1})^\dagger_{33}}{c_\beta\mathbf{V}_{33}}\sum_{j=1,2}\left(-\frac{(C_L)_{i2}(C_R)^*_{i1}M_W}{\sqrt{2}m_{\chi_i^-}}\left|U^{\tilde{t}}_{1j}\right|^2 + (U^{\tilde{t}}_{1j})^*U^{\tilde{t}}_{2j}\frac{(C_L)_{i2}(C_R)^*_{i2}(\hat{\mathbf{M}}_u\mathbf{R}_u^{-1})^\dagger_{33}}{2s_\beta m_{\chi_i^-}}\right)F^{(3)}_{7,8}(x_{\tilde{t}_j\chi_i^-})\Big\}, \end{aligned} \quad (4.16)$$

where $x_{ij} \equiv m_i^2/m_j^2$. We refer to [39] for the functions $F^{(3)}_{7,8}$ and to [40] for the chargino mixing matrices $C_{L,R}$ and the stop mixing matrix $U^{\tilde{t}}$.

Finally, the gluino contributions to the Wilson coefficients $C_{7,8}$ are given by

$$\begin{aligned} C^{\tilde{g}}_7(\mu_{\rm SUSY}) &= -\frac{8\pi\alpha_s}{9\sqrt{2}G_F|M_3|^2\lambda_t}\sum_{i=1}^6 x_i(G^d_L)^*_{i2}\left[(G^d_L)_{i3}f_2(x_i) + (G^d_R)_{i3}\frac{M_3}{m_b}f_4(x_i)\right], \\ C^{\tilde{g}}_8(\mu_{\rm SUSY}) &= -\frac{\pi\alpha_s}{\sqrt{2}G_F|M_3|^2\lambda_t}\sum_{i=1}^6 x_i(G^d_L)^*_{i2}\left\{(G^d_L)_{i3}\left[3f_1(x_i) + \frac{1}{3}f_2(x_i)\right] + (G^d_R)_{i3}\frac{M_3}{m_b}\left[3f_3(x_i) + \frac{1}{3}f_4(x_i)\right]\right\}, \end{aligned} \quad (4.17)$$

where $\lambda_t \equiv \mathbf{V}_{33}\mathbf{V}^\dagger_{23} = V_{tb}V^*_{ts}$ and $x_i \equiv |M_3|^2/m^2_{\tilde{d}_i}$. The loop functions $f_{1,2,3,4}(x_i)$ may be found in Ref. [41]. The Wilson coefficients for the primed operators $\mathcal{O}'_{7,8}$ can be obtained by the exchange $L \leftrightarrow R$ and $M_3 \to M_3^*$:

$$C_7^{l\tilde{g}}(\mu_{\rm SUSY}) = -\frac{8\pi\alpha_s}{9\sqrt{2}G_F|M_3|^2\lambda_t}\sum_{i=1}^{6} x_i (G_R^d)^*_{i2}\Big[(G_R^d)_{i3} f_2(x_i) + (G_L^d)_{i3}\frac{M_3^*}{m_b} f_4(x_i)\Big],$$
$$C_8^{l\tilde{g}}(\mu_{\rm SUSY}) = -\frac{\pi\alpha_s}{\sqrt{2}G_F|M_3|^2\lambda_t}\sum_{i=1}^{6} x_i (G_R^d)^*_{i2}\Big\{(G_R^d)_{i3}\Big[3f_1(x_i) + \frac{1}{3}f_2(x_i)\Big] + (G_L^d)_{i3}\frac{M_3^*}{m_b}\Big[3f_3(x_i) + \frac{1}{3}f_4(x_i)\Big]\Big\}. \tag{4.18}$$

In the above, $C_{7,8}^{(l)\tilde{g}}$, the down-type squark-gluino-quark couplings $G_{L,R}^d$ are defined through the interaction Lagrangian (suppressing the color indices)

$$\mathcal{L}_{\bar{d}\tilde{g}d} = -\sqrt{2}g_s\{\tilde{d}_i^* t^a \tilde{g}^a[(G_L^d)_{i\alpha}P_L + (G_R^d)_{i\alpha}P_R]d_\alpha + \bar{d}_\alpha[(G_L^d)^*_{i\alpha}P_R + (G_R^d)^*_{i\alpha}P_L]\tilde{g}^a t^a \tilde{d}_i\}, \tag{4.19}$$

where t^a are the usual Gell-Mann matrices, $i = 1, 2, \ldots, 6$ label the mass eigenstates of down-type squarks, and $\alpha = 1, 2, 3$ the mass eigenstates of down-type quarks. The couplings are given by the down-type squark mixing matrix as

$$(G_L^d)_{i\alpha} = (U^{\tilde{d}\dagger})_{i\alpha}, \qquad (G_R^d)_{i\alpha} = -(U^{\tilde{d}\dagger})_{i\alpha+3}. \tag{4.20}$$

The 6×6 unitary matrix $U^{\tilde{d}}$ diagonalizes the down-type squark mass matrix as

$$U^{\tilde{d}\dagger}\mathbf{M}_{\tilde{d}}^2 U^{\tilde{d}} = \mathrm{diag}(m_{\tilde{d}_1}^2, m_{\tilde{d}_2}^2, \ldots, m_{\tilde{d}_6}^2), \tag{4.21}$$

where $\tilde{d}_1$ is the lightest and $\tilde{d}_6$ the heaviest. In the super-CKM basis, in which the down squarks are aligned with the down quarks and $\mathbf{U}_L^Q = \mathbf{U}_R^u = \mathbf{U}_R^d = \mathbf{1}$, the 6×6 down-type squark mass matrix $\mathbf{M}_{\tilde{d}}^2$ takes on the form

$$\mathbf{M}_{\tilde{d}}^2 = \begin{pmatrix} \mathbf{V}^\dagger\tilde{\mathbf{M}}_{LL}^2\mathbf{V} & \mathbf{V}^\dagger\tilde{\mathbf{M}}_{LR}^2 \\ \tilde{\mathbf{M}}_{RL}^2\mathbf{V} & \tilde{\mathbf{M}}_{RR}^2 \end{pmatrix}, \tag{4.22}$$

where the 3×3 submatrices are given by

$$\begin{aligned}
\tilde{\mathbf{M}}_{LL}^2 &= \tilde{\mathbf{M}}_Q^2 + \frac{v_1^2}{2}(\mathbf{h}_d^\dagger\mathbf{h}_d) + c_{2\beta}M_Z^2\Big(-\frac{1}{2}+\frac{1}{3}s_W^2\Big)\mathbf{1}, \\
\tilde{\mathbf{M}}_{LR}^2 &= \frac{1}{\sqrt{2}}\mathbf{a}_d^\dagger v_1 - \frac{1}{\sqrt{2}}\mathbf{h}_d^\dagger\mu v_2, \\
\tilde{\mathbf{M}}_{RL}^2 &= \frac{1}{\sqrt{2}}\mathbf{a}_d v_1 - \frac{1}{\sqrt{2}}\mathbf{h}_d\mu^* v_2, \\
\tilde{\mathbf{M}}_{RR}^2 &= \tilde{\mathbf{M}}_D^2 + \frac{v_1^2}{2}(\mathbf{h}_d\mathbf{h}_d^\dagger) + c_{2\beta}M_Z^2\Big(-\frac{1}{3}s_W^2\Big)\mathbf{1},
\end{aligned} \tag{4.23}$$

with $\mathbf{h}_d = \frac{\sqrt{2}}{v_1}\hat{\mathbf{M}}_d\mathbf{V}^\dagger\mathbf{R}_d^{-1}$. As a byproduct of the chosen super-CKM basis, we observe the absence of flavor mixing in $\mathbf{M}_{\tilde{d}}^2$, for all $\mathbf{h}_d$-dependent terms, when $\mathbf{R}_d \propto \mathbf{1}$.

V. NUMERICAL EXAMPLES

For our numerical estimates of FCNC observables at large $\tan\beta$, we take the GUT scale to be the same as in the usual CMSSM with MFV, and a dedicated program has been developed to calculate the RG evolution from the GUT scale to the low-energy SUSY scale in the MCPMFV framework of the MSSM. For the Higgs mass spectrum and the mixing matrix $O_{\alpha i}$ at the $M_{\rm SUSY}$ scale, the code `CPsuperH` [40] has been used. In the calculation of the flavor-changing effective couplings, only the leading contributions have been kept in the single-Higgs-insertion approximation, neglecting the EW corrections and the generically small flavor-off-diagonal elements of the squark mass matrices.

In order to study the effects of *CP*-violating phases in the MCPMFV framework, we consider a *CP*-violating variant of a typical CMSSM scenario:

$$\begin{aligned}
&|M_{1,2,3}| = 250\ \text{GeV}, \\
&M_{H_u}^2 = M_{H_d}^2 = \tilde{M}_Q^2 = \tilde{M}_U^2 = \tilde{M}_D^2 = \tilde{M}_L^2 = \tilde{M}_E^2 \\
&\qquad = (100\ \text{GeV})^2, \\
&|A_u| = |A_d| = |A_e| = 100\ \text{GeV},
\end{aligned} \tag{5.1}$$

at the GUT scale with $\tan\beta(M_{\rm SUSY}) = 10$, which corresponds to $\tan\beta(m_t^{\rm pole}) \simeq 10.2$. As for the *CP*-violating phases, we adopt the convention that $\Phi_\mu = 0°$, and we vary the following three phases:

$$\begin{aligned}
&\Phi_{12} \equiv \Phi_1 = \Phi_2; \qquad \Phi_3; \\
&\Phi_A^{\rm GUT} \equiv \Phi_{A_u} = \Phi_{A_u} = \Phi_{A_e},
\end{aligned} \tag{5.2}$$

where, for simplicity, common phases Φ_{12} and $\Phi_A^{\rm GUT}$ are taken for the phases of $M_{1,2}(M_{\rm GUT})$ and $A_{u,d,e}(M_{\rm GUT})$, respectively. We note that the phases of the gaugino mass parameters, $\Phi_{1,2,3}$, and the μ parameter, Φ_μ, are unchanged by the RG evolution, while the phases of the elements of the matrix $\mathbf{A}_{u,d,e}$ could be significantly different at low scales from the values given at the GUT scale. This scenario becomes the SPS1a point [42] when $\Phi_{1,2,3} = 0°$ and $\Phi_A^{\rm GUT} = 180°$. We have found that $M_{\rm SUSY}$ varies between 530 GeV and 540 GeV, and $M_{\rm GUT}/10^{16}$ GeV between 1.825 and 1.838 depending on the values of the *CP*-violating phases.

We do not consider in this section the electric dipole moment (EDM) constraints [43] on the MCPMFV parameter space of the MSSM. A systematic implementation of these constraints and their impact on the FCNC observables will be given in a forthcoming communication.

A. Phases and masses

We first consider the (3, 3) elements $A_{f_3} \equiv (\mathbf{a}_f)_{33}/(\mathbf{h}_f)_{33}$ at $M_{\rm SUSY}$ with $f = u, d, e$ and $f_3 = t, b, \tau$. We find that the complex quantity A_{f_3} can be written in

terms of the complex A_f and M_j at the GUT scale as:

$$A_{f_3}(M_{\rm SUSY}) \approx C_{f_3}^{A_f} A_f(M_{\rm GUT}) - C_{f_3}^{M_i} M_i(M_{\rm GUT}), \quad (5.3)$$

where the real coefficients $C_{f_3}^{A_f}$ and $C_{f_3}^{M_i}$ are functions of the Yukawa and gauge couplings. This expression is similar to that found in Ref. [44]. In general, $C_{t,b}^{A_{u,d}}$ are much smaller than $C_{t,b}^{M_3}$. Indeed, they are even smaller than $C_{t,b}^{M_{1,2}}$ with $C_t^{A_u} < C_b^{A_d}$. For A_τ, $C_\tau^{A_e}$ is not so much smaller than $C_\tau^{M_{1,2}}$, while $C_\tau^{M_3}$ is negligible. This is because the strong coupling amplifies the influence of M_3, while the large Yukawa couplings suppress those of the A terms via renormalization effects [44]. For the parameter set (5.1) with $\tan\beta = 10$, we observe that the phases $\Phi_{A_t}(M_{\rm SUSY})$ and $\Phi_{A_b}(M_{\rm SUSY})$ are largely determined by Φ_3, whereas the phase $\Phi_{A_\tau}(M_{\rm SUSY})$ is more affected by $\Phi_{1,2}$ than by $\Phi_A^{\rm GUT}$. This situation becomes different for larger values of $\tan\beta$, i.e. we find that $C_\tau^{M_3}$ becomes significant and $C_b^{A_d}$ decreases when $\tan\beta$ increases.

In Fig. 4 we show $\sin\Phi_{A_t}$, $\sin\Phi_{A_b}$, and $\sin\Phi_{A_\tau}$ for the parameter set (5.1) with $\tan\beta(M_{\rm SUSY}) = 10$. In the left frames, we observe that $\Phi_{A_{t,b}}$ and Φ_{A_τ} can be fully generated from Φ_3 and $\Phi_{1,2}$, respectively, even when $A_{u,d,e}$ at the GUT scale are real, $\Phi_A^{\rm GUT} = 180°$. Whilst the dependence of Φ_{A_τ} on Φ_3 is negligible (solid line in the left-lower frame), the dependences of $\Phi_{A_{t,b}}$ on $\Phi_{1,2}$ can be sizeable (dashed lines in the left-upper and left-middle frames). In the right frames, the cases with $\Phi_3 = 0°$ ($\Phi_{A_{t,b}}$) and $\Phi_{12} = 0°$ (Φ_{A_τ}) are considered, showing how large the A-term phases may become at the $M_{\rm SUSY}$ scale for real M_3 and/or real M_1 and M_2. When the gaugino masses are all real, $|\sin\Phi_{A_t}|$ and $|\sin\Phi_{A_b}|$ turn out to be 0.06 and 0.12, respectively, whereas $|\sin\Phi_{A_\tau}|$ can be as large as 0.55. Somewhat larger CP-violating phases are possible for Φ_{A_t} and Φ_{A_b} when M_1 and M_2 are pure imaginary (see dashed and dash-dotted lines in the right-upper and right-middle frames of Fig. 4). Finally, there are no visible effects of Φ_3 on Φ_{A_τ}.

We now discuss the effects of CP-violating phases on the masses of Higgs bosons, third-generation squarks, and

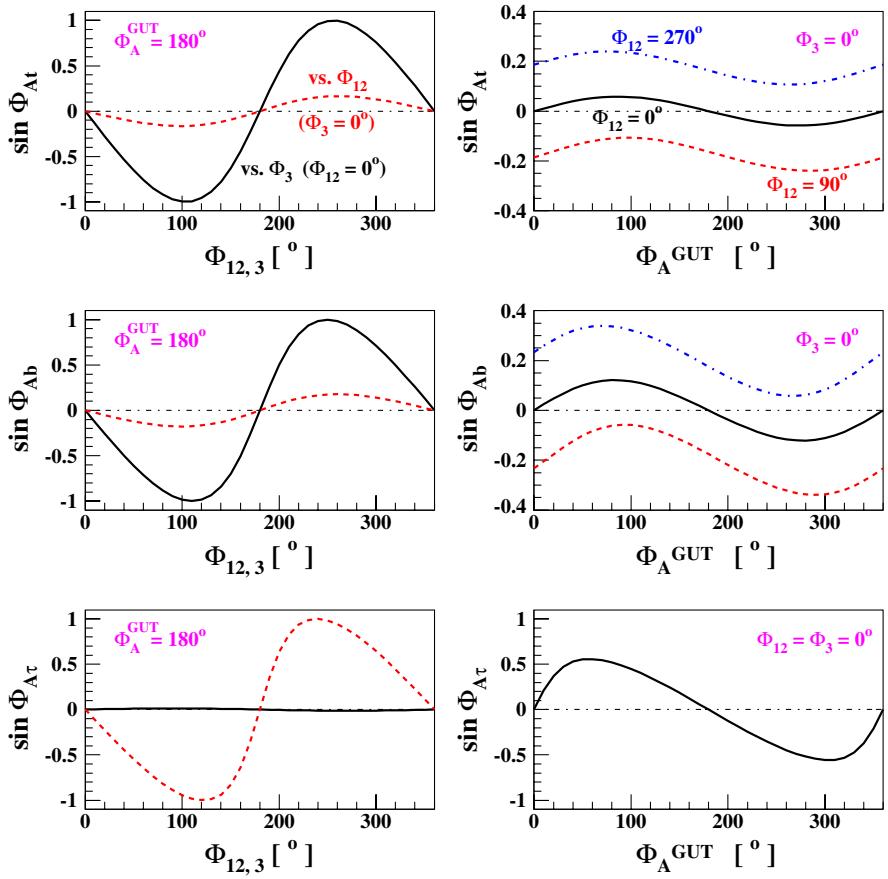

FIG. 4 (color online). In the left frames, taking $\Phi_A^{\rm GUT} = 180°$, $\sin\Phi_{A_t}$ (upper), $\sin\Phi_{A_b}$ (middle), and $\sin\Phi_{A_\tau}$ (lower) are shown as functions of Φ_3 taking $\Phi_{12} = 0°$ (solid lines) and Φ_{12} taking $\Phi_3 = 0°$ (dashed lines). In the right frames they are shown as functions of $\Phi_A^{\rm GUT}$ taking $\Phi_3 = 0°$ or $\Phi_{12} = 0°$. For $\sin\Phi_{A_t}$ and $\sin\Phi_{A_b}$, three cases are shown: $\Phi_{12} = 270°$ (blue dash-dotted lines), 0° (black solid lines), and 90° (red dashed lines). For $\sin\Phi_{A_\tau}$, we set $\Phi_3 = 0°$ as well. The parameters are taken as in Eq. (5.1) with $\tan\beta(M_{\rm SUSY}) = 10$.

heavy neutralinos and chargino. In the upper-left frame of Fig. 5, we show the absolute values of $A_{t,b,\tau}$ as functions of a common phase $\Phi_M \equiv \Phi_1 = \Phi_2 = \Phi_3$ for two values of $\Phi_A^{\rm GUT}$: 0° (dashed lines) and 180° (solid lines). In this case, one can show the absolute values squared depend only on the difference $\Phi_A^{\rm GUT} - \Phi_M$:

$$|A_f|^2 \approx \alpha_f - \beta_f \cos(\Phi_A^{\rm GUT} - \Phi_M), \qquad (5.4)$$

using Eq. (5.3), with α_f, $\beta_f > 0$. From Fig. 5, we observe that there is strong correlation between $|A_{t,b,\tau}|$ and the particle mass spectrum. This correlation is due to the phase-dependent terms $\mathrm{Tr}(\mathbf{a}_u^\dagger \mathbf{a}_u)$ and $\mathrm{Tr}(\mathbf{a}_d^\dagger \mathbf{a}_d)$ in $dM_{H_u,H_d}^2/dt$ and $d\tilde{\mathbf{M}}_{Q,U,D}^2/dt$. The fact that $|M_{H_u}^2|$ decreases (increases) when $\mathrm{Tr}(\mathbf{a}_u^\dagger \mathbf{a}_u)$ decreases (increases) explains the *CP*-odd phase dependence of heavier Higgs-boson masses, as can be seen from the upper-right frame of Fig. 5. The same correlation is observed for the heavy chargino and neutralinos in the lower-right frame of Fig. 5, since a decreased (increased) value of $|M_{H_u}^2|$ leads to smaller (larger) values of $|\mu|$. We find that the variations in the masses of the lightest Higgs boson H_1 and the lightest neutralino $\tilde{\chi}_1^0$ amount to 2 GeV and 3 GeV, respectively. The *CP*-odd phase dependences of $\tilde{\mathbf{M}}_Q^2$, $\tilde{\mathbf{M}}_U^2$, and $\tilde{\mathbf{M}}_D^2$ at the scale $M_{\rm SUSY}$ can be understood similarly. Here the (3, 3) components of the mass matrices decrease (increase) when $\mathrm{Tr}(\mathbf{a}_u^\dagger \mathbf{a}_u)$ increases (decreases). For the chosen value of $\tan\beta(M_{\rm SUSY}) = 10$, the (3, 3) component of $\tilde{\mathbf{M}}_U^2$ shows the largest effect, since $d\tilde{\mathbf{M}}_U^2/dt$ contains $2\,\mathrm{Tr}(\mathbf{a}_u^\dagger \mathbf{a}_u)$ compared to $\mathrm{Tr}(\mathbf{a}_u^\dagger \mathbf{a}_u) + \mathrm{Tr}(\mathbf{a}_d^\dagger \mathbf{a}_d)$ in $d\tilde{\mathbf{M}}_Q^2/dt$ and $2\,\mathrm{Tr}(\mathbf{a}_d^\dagger \mathbf{a}_d)$ in $d\tilde{\mathbf{M}}_D^2/dt$. Furthermore, we note that $\tilde{t}_1 \sim \tilde{t}_R$ and $\tilde{b}_1 \sim \tilde{b}_L$. From these observations, one can understand the qualitative *CP*-odd phase dependence of the stop and sbottom masses, as shown in the lower-left frame of Fig. 5.

B. Effects on ΔM_{B_s} and ΔM_{B_d}

In the upper-left frame of Fig. 6, we show the SUSY contribution to ΔM_{B_s} in units of ps^{-1} as a function of $\tan\beta(M_{\rm SUSY})$ for three values of the common phase, namely $\Phi_M = 0°$ (solid line), 90° (dashed line), and 180° (dash-dotted line). The horizontal line is for the measured value: $\Delta M_{B_s}^{\rm EXP} = 17.77 \pm 0.10(\mathrm{stat.}) \pm 0.07(\mathrm{syst.})\ \mathrm{ps}^{-1}$ [18]. We observe that the SUSY contribution can be larger than the current observed value for

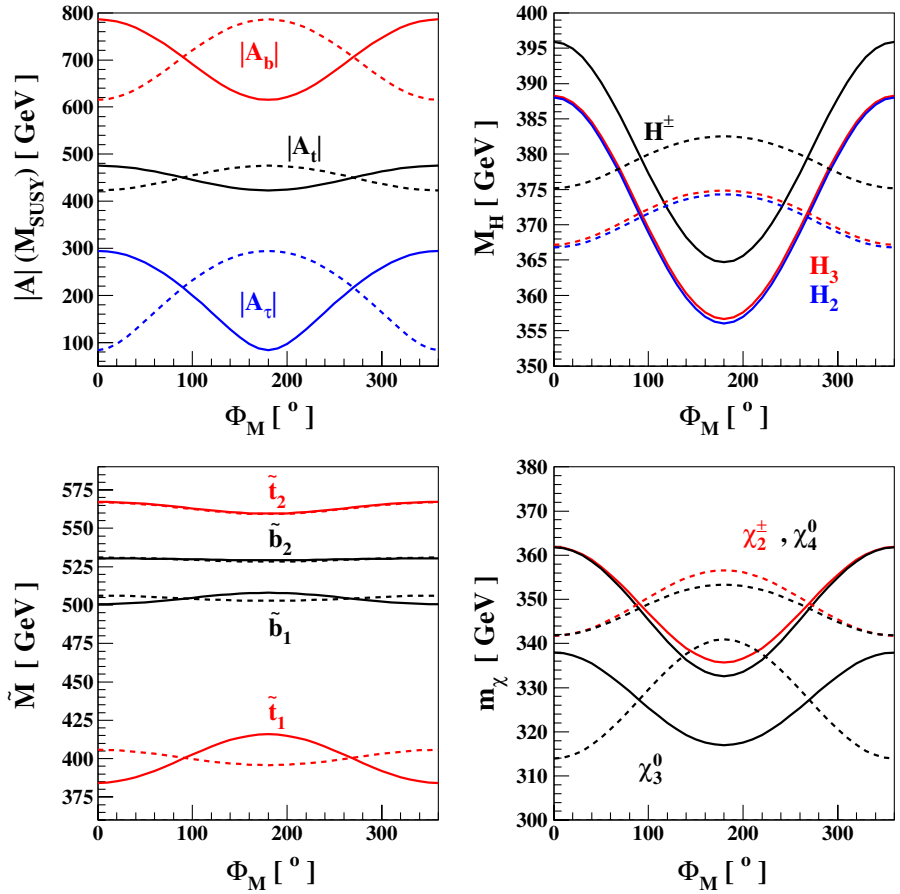

FIG. 5 (color online). The absolute values of $A_{t,b,\tau}$ (upper-left) and the masses of the heavy Higgs bosons (upper-right), sbottoms and stops (lower-left), and charginos and neutralinos (lower-right) as functions of a common phase $\Phi_M = \Phi_1 = \Phi_2 = \Phi_3$. The solid lines are for $\Phi_A^{\rm GUT} = 180°$ and the dashed lines for $\Phi_A^{\rm GUT} = 0°$. The parameters are listed in Eq. (5.1).

$\Phi_M = 180°$ when $\tan\beta$ is large. Indeed, for $\Phi_M = 180°$ (90°), we find $\tan\beta < 44(48)$, whereas there is no restriction on $\tan\beta$ for $\Phi_M = 0°$.

The SUSY contribution $C_1^{\mathrm{SRR(DP)}}$ is suppressed by m_s^2/m_b^2 with respect to $C_1^{\mathrm{SRR(DP)}}$ [see Eq. (4.4)]. The $|C_2^{\mathrm{LR(DP)}}|$ is comparable to $|C_1^{\mathrm{SLL(DP)}}|$, while the 2HDM contribution, $C_2^{\mathrm{LR(2HDM)}}$, becomes less important as $\tan\beta$ increases. The dip of the coupling $|C_1^{\mathrm{SLL(DP)}}|$ for $\Phi_M = 180°$ (upper-right frame) at $\tan\beta \simeq 45$ is due to the fact that the three Higgs bosons become degenerate and cancel other contributions. Beyond this point, $M_{H_1} \sim M_{H_2}$ decreases rapidly while $M_{H_3} \sim 110$ GeV remains nearly unchanged.

In the upper-left frame of Fig. 7, we show the SUSY contribution to ΔM_{B_d} in units of ps^{-1} as a function of $\tan\beta(M_{\mathrm{SUSY}})$, using the same line conventions as in Fig. 6. The horizontal line is for the measured value: $\Delta M_{B_d}^{\mathrm{EXP}} = 0.507 \pm 0.005\ \mathrm{ps}^{-1}$ [45]. We observe that the SUSY contribution is always smaller than the measured value, although it does exhibit a strong dependence on the CP-violating phase Φ_M. The dips at $\tan\beta \simeq 45$ ($\Phi_M = 180°$) and $\tan\beta \simeq 49$ ($\Phi_M = 90°$) arise for the same reason as in the ΔM_{B_s} case. The dominant contribution comes from $C_1^{\mathrm{SLL(DP)}}$, and $C_1^{\mathrm{SRR(DP)}}$ is suppressed by m_d^2/m_b^2. The value of $|C_2^{\mathrm{LR(DP)}}|$ is smaller than that of $|C_1^{\mathrm{SLL(DP)}}|$. Finally, as before, the 2HDM contribution $C_2^{\mathrm{LR(2HDM)}}$ becomes less significant for large values of $\tan\beta$.

C. Effects on $B_s \to \mu^+\mu^-$

In the upper-left frame of Fig. 8, we show the branching ratio $B(B_s \to \mu^+\mu^-)$ as a function of $\tan\beta(M_{\mathrm{SUSY}})$ using the same line conventions as in Fig. 6 for three values of the common phase Φ_M: $\Phi_M = 0°$ (solid line), 90° (dashed line), and 180° (dash-dotted line). The two horizontal lines in the upper-left frame are for the SM prediction and the current upper limit at 90% C.L., namely 7.5×10^{-8} [18]. We observe that the branching ratio changes substantially as Φ_M varies. Specifically, for $\Phi_M = 180°$ (90°) 0°, (we find that the present upper limit on $B(B_s \to \mu^+\mu^-)$ imposes the upper limit $\tan\beta < 34(38)42$.

The phase dependence of the branching ratio comes from that of the couplings C_S and C_P [see (4.8)], which are shown in the upper-right and the lower-left frames, respectively. We find that $|C_S| \simeq |C_P|$, since

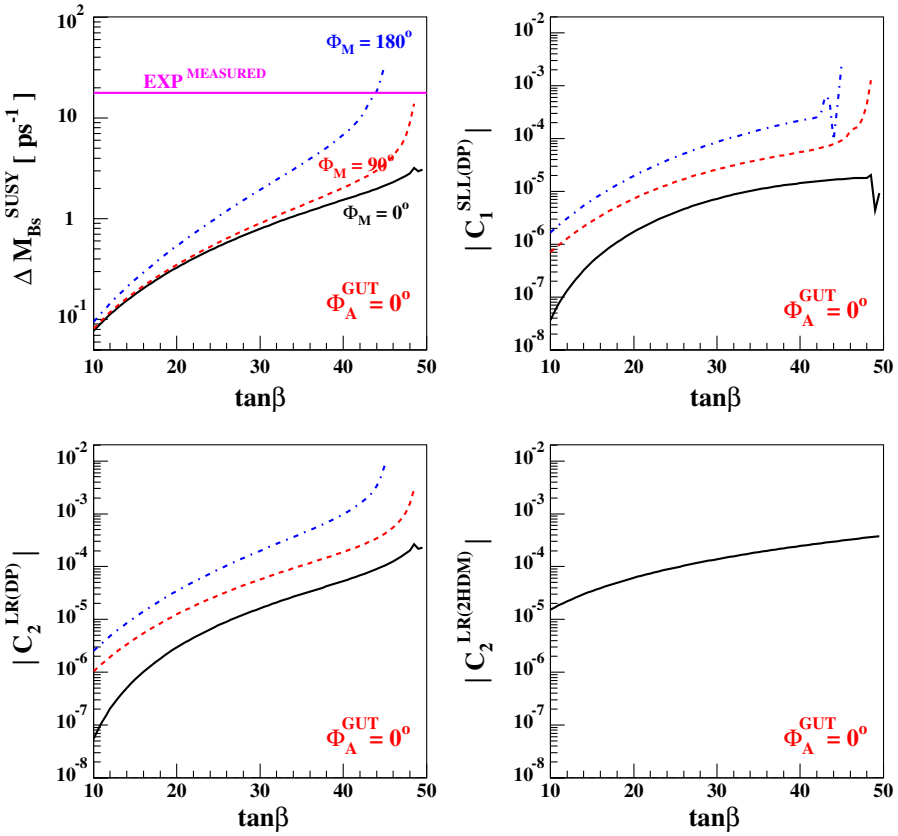

FIG. 6 (color online). The SUSY contribution to ΔM_{B_s} in units of ps^{-1} (upper-left) and the relevant couplings in the other three frames, as functions of $\tan\beta(M_{\mathrm{SUSY}})$, for three values of the common phase: $\Phi_M = 0°$ (solid lines), 90° (dashed lines), and 180° (dash-dotted lines). We fix $\Phi_A^{\mathrm{GUT}} = 0°$ and the parameters are taken as in Eq. (5.1), except that here we choose $\tilde{M}_{L,E} = 200$ GeV so as to avoid a very light or tachyonic $\tilde{\tau}_1$ state for large $\tan\beta$. In the upper-left frame, we show the currently measured value as the horizontal line.

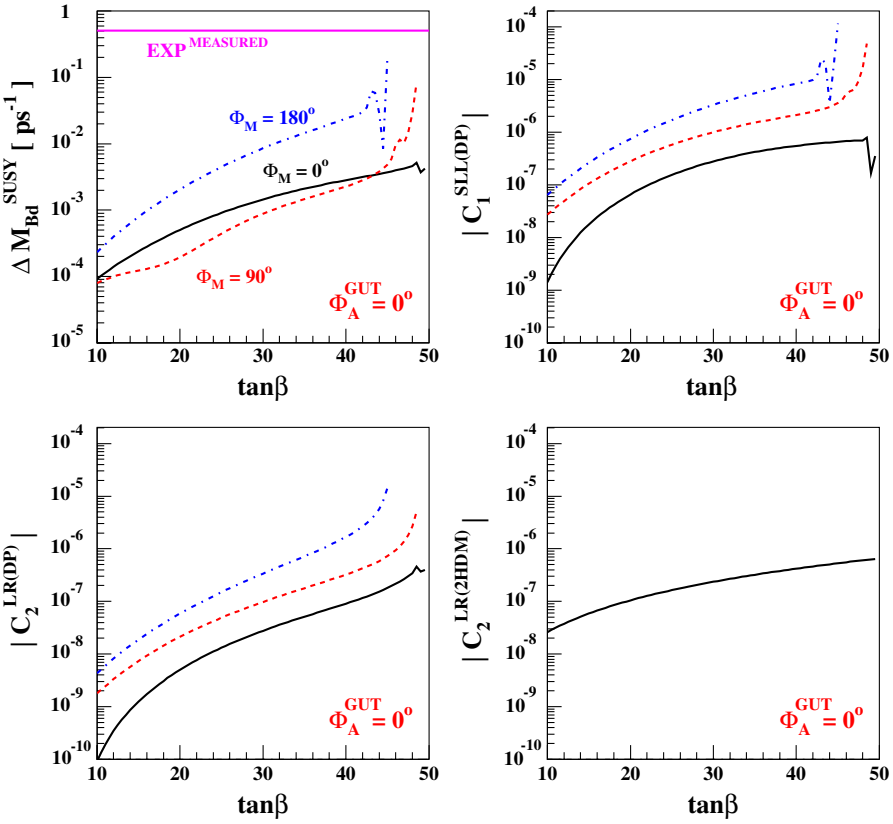

FIG. 7 (color online). The SUSY contribution to ΔM_{B_d} in units of ps^{-1} (upper-left) and the relevant couplings in the other three frames. The line conventions and the parameters are the same as in Fig. 6.

$O_{11} \sim O_{a1} \sim 0$ and $M_{H_2} \sim M_{H_3}$ [cf. (4.8) and (4.9)]. We note that, for $\Phi_M = 180°$, $B(B_s \to \mu^+\mu^-)$ can be smaller than the SM prediction for $\tan\beta \lesssim 24$. This is because the Higgs-mediated contribution C_P cancels the SM one C_{10}, as shown in the lower-right frame of Fig. 8, in which the factor $m_b/(m_b + m_s)$ [cf. (4.11)] has been suppressed in the label of the y-axis.

D. Effects on $B_u \to \tau\nu$

The recent Belle and *BABAR* results for the branching ratio $B(B^- \to \tau^-\bar{\nu})$ are [46,47]

$$B(B^- \to \tau^-\bar{\nu})^{\rm Belle} = (1.79^{+0.56}_{-0.49}({\rm stat})^{+0.46}_{-0.51}({\rm syst})) \times 10^{-4},$$
$$B(B^- \to \tau^-\bar{\nu})^{BABAR} = (1.2 \pm 0.4({\rm stat}) \pm 0.3({\rm bkg\ syst}) \pm 0.2({\rm other\ syst})) \times 10^{-4}, \quad (5.5)$$

which lead to $B(B^- \to \tau^-\bar{\nu})^{\rm EXP} = (1.4 \pm 0.43) \times 10^{-4}$. Combining the Belle and *BABAR* results with the SM value $B(B^- \to \tau^-\bar{\nu})^{\rm SM} = (1.41 \pm 0.33) \times 10^{-4}$ obtained by the global fit without using $B(B^- \to \tau^-\bar{\nu})$ as an input [48], we have the following 1σ range for the ratio to the SM prediction[3]:

$$R^{\rm EXP}_{B\tau\nu} = 1.0 \pm 0.38. \quad (5.6)$$

In the upper-left frame of Fig. 9, we show possible values of this ratio in the MSSM with MCPMFV, together with the experimental range given in (5.6), as functions of $\tan\beta$ for three representative values of the common phase Φ_M and for $\Phi_A^{\rm GUT} = 0$. The three thin arrows at the bottom indicate the positions where the ratio vanishes at the tree level without including threshold corrections for $\Phi_M = 180°$, 90°, and 0° (from left to right). Beyond the minimum point, the charged-Higgs-boson contribution dominates over the SM one. It rapidly grows as $\tan^4\beta$ initially and then goes over to $\tan^2\beta$ due to the threshold corrections. For each displayed value of Φ_M, we find two regions of $\tan\beta$ where the experimental value of $B(B^- \to \tau^-\bar{\nu})$ is obtained. One region is at $\tan\beta < 25$ (27) 29 for $\Phi_M =$ 180° (90°) 0°, and corresponds to the case where the charged-Higgs-boson contribution is a small "correction" to the SM term. The second region is at $\tan\beta \sim 41$ (46) 48, for $\Phi_M = 180°$ (90°) 0°, and corresponds to the case where the charged-Higgs-boson contribution dominates over the SM term. We note that the locations of these second allowed regions would not be estimated correctly if the threshold corrections were not included. These regions are actually excluded by the $B_s \to \mu^+\mu^-$ constraint discussed previously.

[3]This range is different from that used in [49] due to the new *BABAR* result [47].

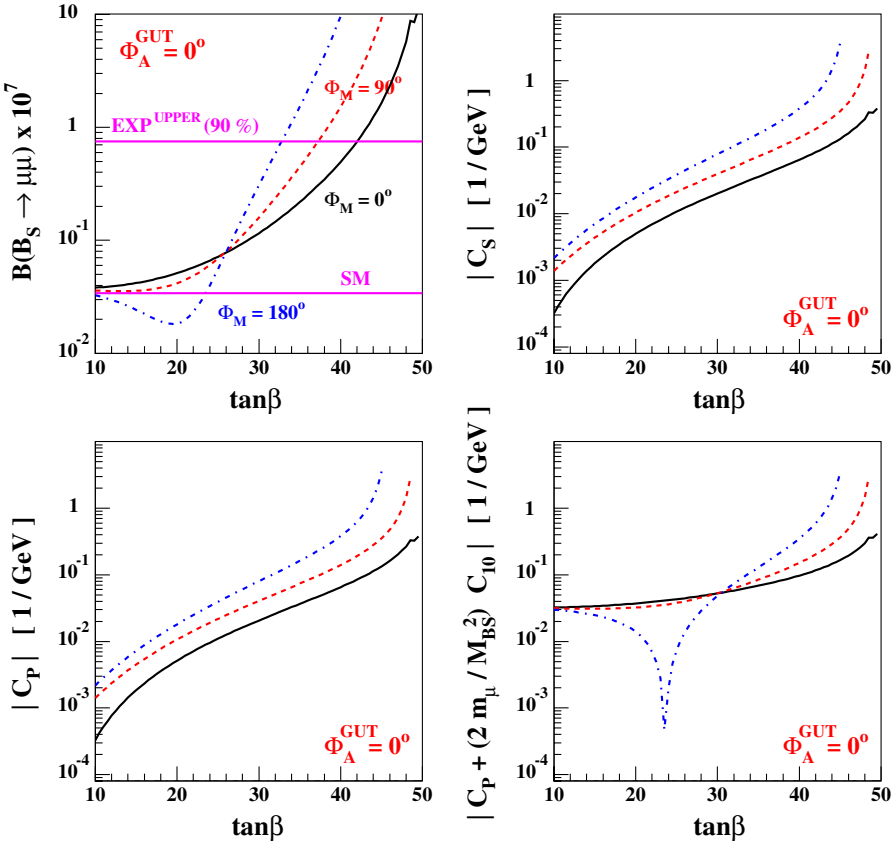

FIG. 8 (color online). The branching ratio $B(B_s \to \mu^+\mu^-)$ in the upper-left frame and the relevant couplings in the other three frames, in units of GeV^{-1} as functions of $\tan\beta(M_{\mathrm{SUSY}})$. The line conventions and the parameters chosen are the same as in Fig. 6, except that the two horizontal lines in the upper-left frame are for the SM prediction and the current upper limit at 90% C.L.

The tree-level vanishing points are also indicated in the upper-right frame as intersections of the $M_{H^\pm}$ and $\tan\beta \times M_{B^\pm}$ lines. We observe that the resummed threshold effects enhance the charged-Higgs-boson contribution when $\Phi_M = 180°$ and suppress it when $\Phi_M = 0°$. As can be seen from the lower-left frame of Fig. 9, for $\Phi_M = 90°$, the $\tan\beta$ dependence of $R_{B\tau\nu}$ becomes rather similar to the tree-level one. However, as displayed in the lower-right frame of Fig. 9, there is a nonvanishing contribution from the imaginary part of the coupling $(\mathbf{g}^{L\dagger}_{H^-\bar{d}u})_{13}/\mathbf{V}_{13}$.

E. Effects on $B \to X_s\gamma$

The current experimental bound on $B(B \to X_s\gamma)$ with a photon energy cut of $E_\gamma > E_{\mathrm{cut}} = 1.6$ GeV is [50]

$$B(B \to X_s\gamma)^{\mathrm{EXP}} = (3.55 \pm 0.24^{+0.09}_{-0.10} \pm 0.03) \times 10^{-4}. \tag{5.7}$$

Our estimate of the SM prediction based on the NLO calculation is 3.35×10^{-4}, which is about 1σ larger than the NNLO result, $(3.15 \pm 0.23) \times 10^{-4}$ [36]. In Fig. 10 we show the branching ratio $B(B \to X_s\gamma)$ and the direct CP asymmetry $\mathcal{A}^{\mathrm{dir}}_{\mathrm{CP}}(B \to X_s\gamma)$ as functions of $\tan\beta$. In the upper-left frame, we include only the charged-Higgs contribution, which increases the branching ratio. The larger contribution in the high-$\tan\beta$ region is due to the decrease of the charged-Higgs-boson mass. In the upper-right frame of Fig. 10, we add the contribution from the chargino-mediated loops. This contribution largely cancels the charged-Higgs contribution, when $\Phi_M \lesssim 90°$. Instead, if Φ_M is larger than $\sim 90°$, the chargino contribution interferes constructively with the SM one, resulting in a rapid increase of the branching ratio as $\tan\beta$ grows. This behavior can be understood from the fact that the dominant contribution to $C^{\chi^\pm}_{7,8}$ comes from the last term of Eq. (4.16), which is proportional to $\sim e^{i\Phi_{A_t}}/c_\beta$, and the branching ratio is proportional to its real part, namely $\cos\Phi_{A_t}/c_\beta$. We recall that the phase Φ_{A_t} at the low-energy scale can largely be induced by nonvanishing Φ_M even when Φ^{GUT}_A vanishes (see the upper frames of Fig. 4). In the lower-left frame of Fig. 10, we show the full result including the contribution of the gluino-mediated loops, which is nonvanishing in the presence of flavor mixing in the down-type squark mass matrix. We find that it is numerically negligible for the parameters chosen. In the same frame, as well as in the upper-right one, we show the case of the common phase $\Phi_M = 60°$, in which there is a nearly exact cancellation between the chargino and charged-Higgs con-

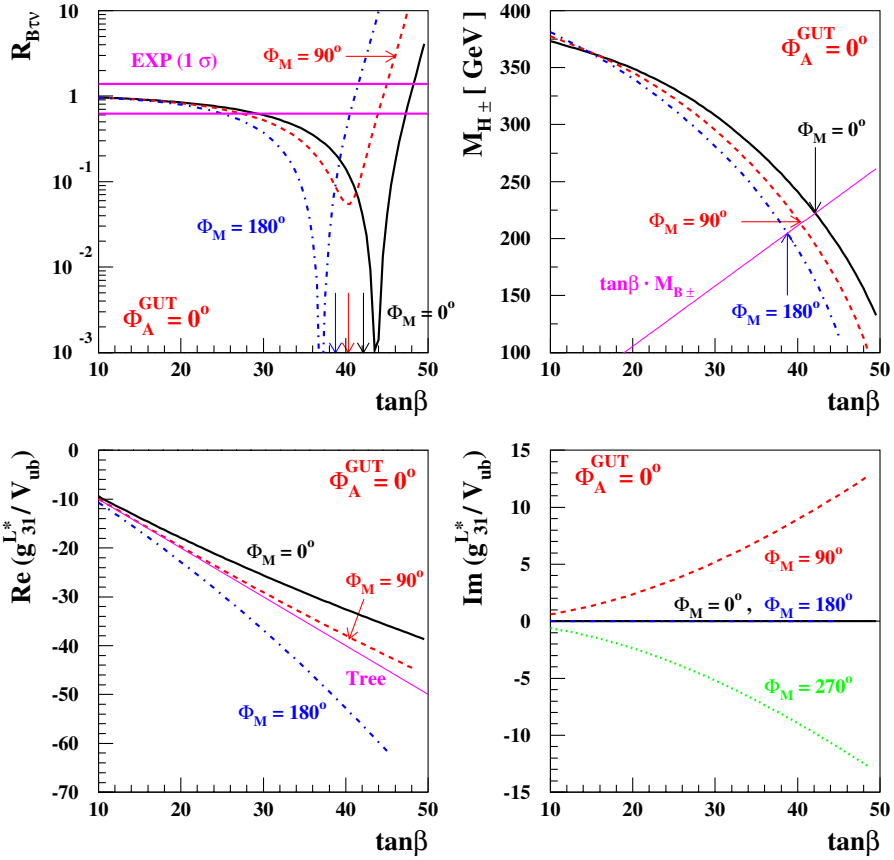

FIG. 9 (color online). The ratio $R_{B\tau\nu}$ (upper-left), the charged-Higgs-boson mass in GeV (upper-right), and the real (lower-left) and imaginary (lower-right) parts of the coupling $(\mathbf{g}^{L\dagger}_{H-\bar{d}u})_{13}/\mathbf{V}_{13} = (\mathbf{g}^{L*}_{H-\bar{d}u})_{31}/V_{ub}$ as functions of $\tan\beta$ for three or four values of Φ_M, taking $\Phi_A^{\rm GUT} = 0°$. The experimentally allowed 1-σ region is bounded with two horizontal lines in the upper-left frame. The straight line with a tag "Tree" in the lower-left frame shows the tree-level coupling. The parameters are the same as in Fig. 6.

tributions, and all the $\tan\beta$ region considered is compatible with the current experimental bound. This observation is also apparent in the left panel of Fig. 11. In the lower-right frame of Fig. 10, we show the direct *CP* asymmetry for several combinations of $(\Phi_A^{\rm GUT}, \Phi_M)$, finding that it can be as large as $\sim -4\%$, when $\Phi_M = 60°$.

To illustrate the strong dependences of the branching ratio and the *CP* asymmetry on the common phase Φ_M, we show them as functions of Φ_M for four values of $\tan\beta$ in Fig. 11. The region allowed experimentally at the 2-σ level is bounded by two horizontal lines in the left frame. In the right frame, points within this region are denoted with open squares. We observe that the branching ratio is quite insensitive to $\tan\beta$ around $\Phi_M = 60°$, whereas the *CP* asymmetry can be as large as $\pm 5\%$ for points within the current 2-σ bound on the branching ratio. For comparison, we note that the experimental range currently allowed is $0.4 \pm 3.7\%$ [50], implying that the new contribution in the MSSM with MCPMFV could be comparable to the present experimental error, and much larger than the SM contribution, which is expected to be below 1%. Finally, it is important to remark that, in the absence of any cancellation mechanism [43], EDM constraints severely restrict the soft *CP*-odd phases in constrained models of low-scale SUSY, such as the constrained MSSM. In a forthcoming paper, however, we will demonstrate in detail, how these constraints can be considerably relaxed in the MSSM with MCPMFV.

VI. CONCLUSIONS

In this paper we have formulated the maximally *CP*-violating version of the MSSM with minimal flavor violation, the MSSM with MCPMFV, showing that it has 19 parameters, including 6 additional *CP*-violating phases beyond the CKM phase in the SM. As preparation for our discussion of *B*-meson observables, we have developed a manifestly flavor-covariant effective Lagrangian formalism, including a new class of dominant subleading contributions due to nondecoupling effects of the third-generation quarks. We have presented analytical results for a range of different *B*-meson observables, including the B_s and B_d mass differences, and the decays $B_s \to \mu^+\mu^-$, $B_u \to \tau\nu$, and $b \to s\gamma$. We have presented numerical results for these observables in one specific MCPMFV scenario. This serves to demonstrate that the experimental

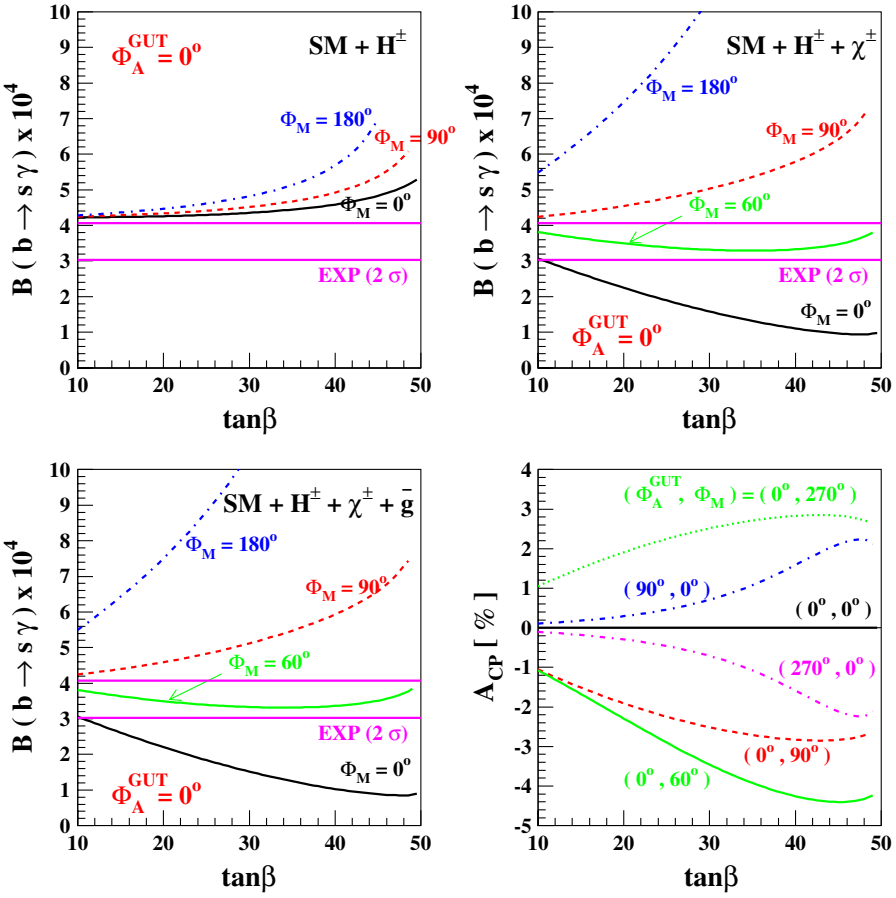

FIG. 10 (color online). The branching ratio $B(B \to X_s\gamma)$ as a function of $\tan\beta$ for several values of the common phase $\Phi_M = \Phi_1 = \Phi_2 = \Phi_3$ and $\Phi_A^{\rm GUT}$. The region allowed experimentally at the 2-σ level is bounded by two horizontal lines. In the upper-left frame, only the charged-Higgs contribution is added to the SM prediction. In the upper-right and lower-left frames, the SUSY contributions are included. The direct CP asymmetry $\mathcal{A}_{\rm CP}^{\rm dir}(B \to X_s\gamma)$ is also shown in the lower-right frame for several combinations of $(\Phi_A^{\rm GUT}, \Phi_M)$. The parameters are the same as in Fig. 6.

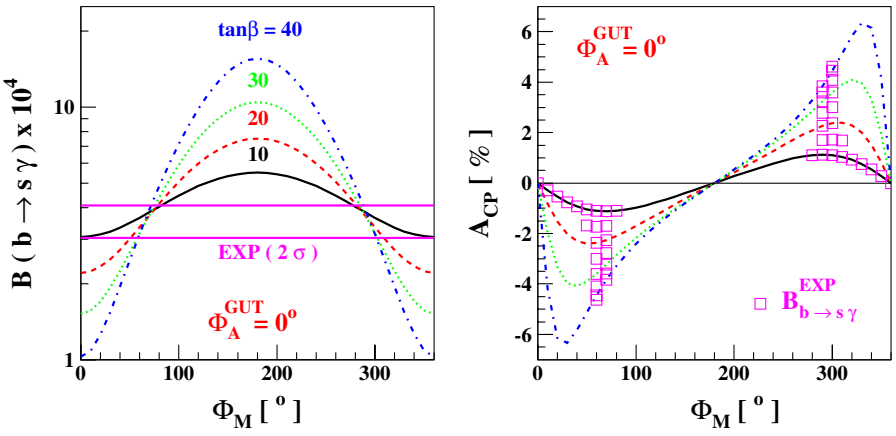

FIG. 11 (color online). The branching ratio $B(B \to X_s\gamma)$ (left) and the CP asymmetry $\mathcal{A}_{\rm CP}^{\rm dir}(B \to X_s\gamma)$ (right) as functions of Φ_M for four values of $\tan\beta$ taking $\Phi_A^{\rm GUT} = 0°$. The region allowed experimentally at the 2-σ level is bounded by two horizontal lines in the left frame. In the right frame, points satisfying this constraint are denoted by open squares. The parameters are the same as in Fig. 6.

constraints on B-meson mixings and their decays impose constraints, e.g., on $\tan\beta$, that depend strongly on the CP-violating phases in the MCPMFV model, most notably on the soft gluino-mass phase in the specific example studied.

In summary, on the one hand, our paper introduces a new class of MSSM models of potential phenomenological interest and develops an appropriate formalism for analyzing them, and on the other, it presents exploratory numerical studies of the constraints imposed by experimental limits on B-meson observables. In view of the large number of the theoretical parameters in the MSSM with MCPMFV, we leave for future work a more complete exploration of its parameter space, including the correlation with other experimental constraints, e.g. those imposed by limits on electric dipole moments.

ACKNOWLEDGMENTS

The work of A. P. has been supported in part by the STFC Research Grant No. PP/D000157/1. The work of J. S. L. has been supported in part by the Korea Research Foundation and the Korean Federation of Science and Technology Societies Grant funded by the Korea Government (MOEHRD, Basic Research Promotion Fund).

APPENDIX A: RENORMALIZATION GROUP EQUATIONS

Here we list all relevant one-loop renormalization group equations (RGEs) for the gauge and Yukawa couplings [51], as well as for the soft SUSY-breaking mass parameters of the general MSSM [52,53]. Defining the RG evolution parameter $t = \ln(Q^2/M_{\rm GUT}^2)$, we may write down the one-loop RGEs as follows[4]:

$$\frac{dg_{1,2,3}}{dt} = \frac{1}{32\pi^2}\left\{\frac{33}{5}g_1^3, g_2^3, -3g_3^3\right\}, \tag{A1}$$

$$\frac{dM_{1,2,3}}{dt} = \frac{1}{16\pi^2}\left\{\frac{33}{5}g_1^2M_1, g_2^2M_2, -3g_3^2M_3\right\}, \tag{A2}$$

$$\frac{d\mathbf{h}_u}{dt} = \frac{\mathbf{h}_u}{32\pi^2}\left(-\frac{13}{15}g_1^2 - 3g_2^2 - \frac{16}{3}g_3^2 + 3\mathbf{h}_u^\dagger\mathbf{h}_u + \mathbf{h}_d^\dagger\mathbf{h}_d + 3\,\mathrm{Tr}(\mathbf{h}_u^\dagger\mathbf{h}_u)\right), \tag{A3}$$

$$\frac{d\mathbf{h}_d}{dt} = \frac{\mathbf{h}_d}{32\pi^2}\left(-\frac{7}{15}g_1^2 - 3g_2^2 - \frac{16}{3}g_3^2 + 3\mathbf{h}_d^\dagger\mathbf{h}_d + \mathbf{h}_u^\dagger\mathbf{h}_u + 3\,\mathrm{Tr}(\mathbf{h}_d^\dagger\mathbf{h}_d) + \mathrm{Tr}(\mathbf{h}_e^\dagger\mathbf{h}_e)\right), \tag{A4}$$

$$\frac{d\mathbf{h}_e}{dt} = \frac{\mathbf{h}_e}{32\pi^2}\left(-\frac{9}{5}g_1^2 - 3g_2^2 + 3\mathbf{h}_e^\dagger\mathbf{h}_e + 3\,\mathrm{Tr}(\mathbf{h}_d^\dagger\mathbf{h}_d) + \mathrm{Tr}(\mathbf{h}_e^\dagger\mathbf{h}_e)\right), \tag{A5}$$

$$\frac{d\mathbf{a}_u}{dt} = \frac{1}{32\pi^2}\left[\left(\frac{26}{15}g_1^2M_1 + 6g_2^2M_2 + \frac{32}{3}g_3^2M_3\right)\mathbf{h}_u - \left(\frac{13}{15}g_1^2 + 3g_2^2 + \frac{16}{3}g_3^2\right)\mathbf{a}_u + 4\mathbf{h}_u\mathbf{h}_u^\dagger\mathbf{a}_u + 5\mathbf{a}_u\mathbf{h}_u^\dagger\mathbf{h}_u + 6\,\mathrm{Tr}(\mathbf{h}_u^\dagger\mathbf{a}_u)\mathbf{h}_u + 3\,\mathrm{Tr}(\mathbf{h}_u^\dagger\mathbf{h}_u)\mathbf{a}_u + 2\mathbf{h}_u\mathbf{h}_d^\dagger\mathbf{a}_d + \mathbf{a}_u\mathbf{h}_d^\dagger\mathbf{h}_d\right], \tag{A6}$$

$$\frac{d\mathbf{a}_d}{dt} = \frac{1}{32\pi^2}\left[\left(\frac{14}{15}g_1^2M_1 + 6g_2^2M_2 + \frac{32}{3}g_3^2M_3\right)\mathbf{h}_d - \left(\frac{7}{15}g_1^2 + 3g_2^2 + \frac{16}{3}g_3^2\right)\mathbf{a}_d + 4\mathbf{h}_d\mathbf{h}_d^\dagger\mathbf{a}_d + 5\mathbf{a}_d\mathbf{h}_d^\dagger\mathbf{h}_d + 6\,\mathrm{Tr}(\mathbf{h}_d^\dagger\mathbf{a}_d)\mathbf{h}_d + 3\,\mathrm{Tr}(\mathbf{h}_d^\dagger\mathbf{h}_d)\mathbf{a}_d + 2\mathbf{h}_d\mathbf{h}_u^\dagger\mathbf{a}_u + \mathbf{a}_d\mathbf{h}_u^\dagger\mathbf{h}_u + 2\,\mathrm{Tr}(\mathbf{h}_e^\dagger\mathbf{a}_e)\mathbf{h}_d + \mathrm{Tr}(\mathbf{h}_e^\dagger\mathbf{h}_e)\mathbf{a}_d\right], \tag{A7}$$

$$\frac{d\mathbf{a}_e}{dt} = \frac{1}{32\pi^2}[(6g_1^2M_1 + 6g_2^2M_2)\mathbf{h}_e - (3g_1^2 + 3g_2^2)\mathbf{a}_e + 4\mathbf{h}_e\mathbf{h}_e^\dagger\mathbf{a}_e + 5\mathbf{a}_e\mathbf{h}_e^\dagger\mathbf{h}_e + 2\,\mathrm{Tr}(\mathbf{h}_e^\dagger\mathbf{a}_e)\mathbf{h}_e + \mathrm{Tr}(\mathbf{h}_e^\dagger\mathbf{h}_e)\mathbf{a}_e + 6\,\mathrm{Tr}(\mathbf{h}_d^\dagger\mathbf{a}_d)\mathbf{h}_e + 3\,\mathrm{Tr}(\mathbf{h}_d^\dagger\mathbf{h}_d)\mathbf{a}_e], \tag{A8}$$

$$\frac{dB}{dt} = \frac{3}{16\pi^2}\left(\frac{1}{5}g_1^2M_1 + g_2^2M_2 + \mathrm{Tr}(\mathbf{h}_u^\dagger\mathbf{a}_u) + \mathrm{Tr}(\mathbf{h}_d^\dagger\mathbf{a}_d) + \frac{1}{3}\,\mathrm{Tr}(\mathbf{h}_e^\dagger\mathbf{a}_e)\right), \tag{A9}$$

$$\frac{d\mu}{dt} = \frac{3\mu}{32\pi^2}\left(-\frac{1}{5}g_1^2 - g_2^2 + \mathrm{Tr}(\mathbf{h}_u^\dagger\mathbf{h}_u) + \mathrm{Tr}(\mathbf{h}_d^\dagger\mathbf{h}_d) + \frac{1}{3}\,\mathrm{Tr}(\mathbf{h}_e^\dagger\mathbf{h}_e)\right), \tag{A10}$$

$$\frac{dM_{H_u}^2}{dt} = \frac{3}{16\pi^2}\left(-\frac{1}{5}g_1^2|M_1|^2 - g_2^2|M_2|^2 + \mathrm{Tr}(\mathbf{h}_u\tilde{\mathbf{M}}_Q^2\mathbf{h}_u^\dagger) + \mathrm{Tr}(\mathbf{h}_u^\dagger\tilde{\mathbf{M}}_U^2\mathbf{h}_u) + M_{H_u}^2\,\mathrm{Tr}(\mathbf{h}_u^\dagger\mathbf{h}_u) + \mathrm{Tr}(\mathbf{a}_u^\dagger\mathbf{a}_u) + \frac{1}{10}g_1^2\,\mathrm{Tr}(Y\mathbf{M}^2)\right), \tag{A11}$$

[4]Our results are in agreement with [53].

$$\frac{dM_{H_d}^2}{dt} = \frac{3}{16\pi^2}\Big(-\frac{1}{5}g_1^2|M_1|^2 - g_2^2|M_2|^2 + \mathrm{Tr}(\mathbf{h}_d\tilde{\mathbf{M}}_Q^2\mathbf{h}_d^\dagger) + \mathrm{Tr}(\mathbf{h}_d^\dagger\tilde{\mathbf{M}}_D^2\mathbf{h}_d) + M_{H_d}^2\,\mathrm{Tr}(\mathbf{h}_d^\dagger\mathbf{h}_d) + \mathrm{Tr}(\mathbf{a}_d^\dagger\mathbf{a}_d) + \frac{1}{3}\mathrm{Tr}(\mathbf{h}_e\tilde{\mathbf{M}}_L^2\mathbf{h}_e^\dagger) + \frac{1}{3}\mathrm{Tr}(\mathbf{h}_e^\dagger\tilde{\mathbf{M}}_E^2\mathbf{h}_e) + \frac{1}{3}M_{H_d}^2\,\mathrm{Tr}(\mathbf{h}_e^\dagger\mathbf{h}_e) + \frac{1}{3}\mathrm{Tr}(\mathbf{a}_e^\dagger\mathbf{a}_e) - \frac{1}{10}g_1^2\,\mathrm{Tr}(Y\mathbf{M}^2)\Big), \tag{A12}$$

$$\frac{d\tilde{\mathbf{M}}_Q^2}{dt} = \frac{1}{16\pi^2}\Big[-\Big(\frac{1}{15}g_1^2|M_1|^2 + 3g_2^2|M_2|^2 + \frac{16}{3}g_3^2|M_3|^2\Big)\mathbf{1}_3 + \frac{1}{2}\mathbf{h}_u^\dagger\mathbf{h}_u\tilde{\mathbf{M}}_Q^2 + \frac{1}{2}\tilde{\mathbf{M}}_Q^2\mathbf{h}_u^\dagger\mathbf{h}_u + \mathbf{h}_u^\dagger\tilde{\mathbf{M}}_U^2\mathbf{h}_u + M_{H_u}^2\mathbf{h}_u^\dagger\mathbf{h}_u + \mathbf{a}_u^\dagger\mathbf{a}_u + \frac{1}{2}\mathbf{h}_d^\dagger\mathbf{h}_d\tilde{\mathbf{M}}_Q^2 + \frac{1}{2}\tilde{\mathbf{M}}_Q^2\mathbf{h}_d^\dagger\mathbf{h}_d + \mathbf{h}_d^\dagger\tilde{\mathbf{M}}_D^2\mathbf{h}_d + M_{H_d}^2\mathbf{h}_d^\dagger\mathbf{h}_d + \mathbf{a}_d^\dagger\mathbf{a}_d + \frac{1}{10}g_1^2\,\mathrm{Tr}(Y\mathbf{M}^2)\mathbf{1}_3\Big], \tag{A13}$$

$$\frac{d\tilde{\mathbf{M}}_L^2}{dt} = \frac{1}{16\pi^2}\Big[-\Big(\frac{3}{5}g_1^2|M_1|^2 + 3g_2^2|M_2|^2\Big)\mathbf{1}_3 + \frac{1}{2}\mathbf{h}_e^\dagger\mathbf{h}_e\tilde{\mathbf{M}}_L^2 + \frac{1}{2}\tilde{\mathbf{M}}_L^2\mathbf{h}_e^\dagger\mathbf{h}_e + \mathbf{h}_e^\dagger\tilde{\mathbf{M}}_E^2\mathbf{h}_e + M_{H_d}^2\mathbf{h}_e^\dagger\mathbf{h}_e + \mathbf{a}_e^\dagger\mathbf{a}_e - \frac{3}{10}g_1^2\,\mathrm{Tr}(Y\mathbf{M}^2)\mathbf{1}_3\Big], \tag{A14}$$

$$\frac{d\tilde{\mathbf{M}}_U^2}{dt} = \frac{1}{16\pi^2}\Big[-\Big(\frac{16}{15}g_1^2|M_1|^2 + \frac{16}{3}g_3^2|M_3|^2\Big)\mathbf{1}_3 + \mathbf{h}_u\mathbf{h}_u^\dagger\tilde{\mathbf{M}}_U^2 + \tilde{\mathbf{M}}_U^2\mathbf{h}_u\mathbf{h}_u^\dagger + 2\mathbf{h}_u\tilde{\mathbf{M}}_Q^2\mathbf{h}_u^\dagger + 2M_{H_u}^2\mathbf{h}_u\mathbf{h}_u^\dagger + 2\mathbf{a}_u\mathbf{a}_u^\dagger - \frac{2}{5}g_1^2\,\mathrm{Tr}(Y\mathbf{M}^2)\mathbf{1}_3\Big], \tag{A15}$$

$$\frac{d\tilde{\mathbf{M}}_D^2}{dt} = \frac{1}{16\pi^2}\Big[-\Big(\frac{4}{15}g_1^2|M_1|^2 + \frac{16}{3}g_3^2|M_3|^2\Big)\mathbf{1}_3 + \mathbf{h}_d\mathbf{h}_d^\dagger\tilde{\mathbf{M}}_D^2 + \tilde{\mathbf{M}}_D^2\mathbf{h}_d\mathbf{h}_d^\dagger + 2\mathbf{h}_d\tilde{\mathbf{M}}_Q^2\mathbf{h}_d^\dagger + 2M_{H_d}^2\mathbf{h}_d\mathbf{h}_d^\dagger + 2\mathbf{a}_d\mathbf{a}_d^\dagger + \frac{1}{5}g_1^2\,\mathrm{Tr}(Y\mathbf{M}^2)\mathbf{1}_3\Big], \tag{A16}$$

$$\frac{d\tilde{\mathbf{M}}_E^2}{dt} = \frac{1}{16\pi^2}\Big(-\frac{12}{5}g_1^2|M_1|^2\mathbf{1}_3 + \mathbf{h}_e\mathbf{h}_e^\dagger\tilde{\mathbf{M}}_E^2 + \tilde{\mathbf{M}}_E^2\mathbf{h}_e\mathbf{h}_e^\dagger + 2\mathbf{h}_e\tilde{\mathbf{M}}_L^2\mathbf{h}_e^\dagger + 2M_{H_d}^2\mathbf{h}_e\mathbf{h}_e^\dagger + 2\mathbf{a}_e\mathbf{a}_e^\dagger + \frac{3}{5}g_1^2\,\mathrm{Tr}(Y\mathbf{M}^2)\mathbf{1}_3\Big), \tag{A17}$$

where g_1 is the GUT-normalized gauge coupling, which is related to the $\mathrm{U}(1)_Y$ gauge coupling g' of the SM through $g_1 = \sqrt{5/3}g'$. In addition, the expression

$$\mathrm{Tr}(Y\mathbf{M}^2) = M_{H_u}^2 - M_{H_d}^2 + \mathrm{Tr}(\tilde{\mathbf{M}}_Q^2 - \tilde{\mathbf{M}}_L^2 - 2\tilde{\mathbf{M}}_U^2 + \tilde{\mathbf{M}}_D^2 + \tilde{\mathbf{M}}_E^2) \tag{A18}$$

is the Fayet-Iliopoulos D-term contribution to the one-loop RGEs. It can be shown that $d\,\mathrm{Tr}(Y\mathbf{M}^2)/dt \propto \mathrm{Tr}(Y\mathbf{M}^2)$, i.e., the expression $\mathrm{Tr}(Y\mathbf{M}^2)$ is multiplicatively renormalizable. As usual, the GUT scale is determined by the boundary condition: $g_1(M_{\mathrm{GUT}}) = g_2(M_{\mathrm{GUT}}) = g_3(M_{\mathrm{GUT}})$. We note, finally, that the one-loop RGEs listed above are invariant under the unitary flavor transformations given in (2.5).

APPENDIX B: Z- AND $W^\pm$-BOSON WARD IDENTITIES

In the absence of gauge quantum corrections, the Z- and $W^\pm$ boson couplings to quarks obey the following tree-level WIs [54]:

$$\frac{q^\mu}{M_Z}i\Gamma_\mu^{Zff'}(q,p,p-q) + \Gamma^{G^0ff'}(q,p,p-q) = \frac{ig_w}{M_Z c_w}[(T_z^{f'}P_L - 2Q_{f'}s_w^2)\Sigma_{ff'}(p) - (T_z^f P_R - 2Q_f s_w^2)\Sigma_{ff'}(p-q)], \tag{B1}$$

$$\frac{q^\mu}{M_W}i\Gamma_\mu^{W^+ud}(q,p,p-q) + i\Gamma^{G^+ud}(q,p,p-q) = -\frac{ig_w}{M_W}[\mathbf{V}_{u'd}\Sigma_{uu'}(p)P_L - \mathbf{V}_{ud'}P_R\Sigma_{dd'}(p-q)], \tag{B2}$$

where $c_w = \sqrt{1-s_w^2}$ is the cosine of the weak mixing angle and $T_z^{u(d)} = \frac{1}{2}(-\frac{1}{2})$ and $Q_{u(d)} = \frac{2}{3}(-\frac{1}{3})$ are the weak isospin and electric charge quantum numbers for the u and d quarks. In (B1) and (B2), $\Sigma_{ff'}(p)$ are quark self-energies describing the fermionic transition $f' \to f$, with $f = u, d$ and $f' = u', d'$. In addition, $\Gamma_\mu^{Zff'}(q,p,p-q)$ and $\Gamma_\mu^{W^+ud}(q,p,p-q)$ are vertex functions that describe the interaction of the Z and W^+ boson to quarks, respectively. The momenta q^μ of the gauge bosons are defined as flowing into the vertex, while the momentum flow of the quarks follows the fermion arrow, where p^μ always denotes the outgoing momentum.

In general, virtual strong and electroweak gauge corrections to the Z- and $W^\pm$-boson vertices usually distort these identities, through terms that depend on the gauge-fixing parameter, e.g., ξ. One possible framework in which these identities can be enforced is the pinch technique [55], leading to analytic results that are independent of ξ. Recently, this approach has been extended to super Yang-Mills theories [56]. We ignore the gauge quantum correc-

tions in our phenomenological analysis, since they are rather small.

In the limit $q^\mu \to 0$, the WIs (B1) and (B2) simplify considerably. Let us first consider the WI involving the Z boson and its associate would-be Goldstone boson G^0. Since the vertex function $\Gamma_\mu^{Zff'}(q, p, p-q)$ has no IR singularities in the limit $q^\mu \to 0$, the WI (B1) takes on the much simpler form

$$\Gamma^{G^0 ff'}(0, p, p) = \frac{ig_w}{M_Z c_w} T_z^f [\Sigma_{ff'}(p) P_L - P_R \Sigma_{ff'}(p)]. \tag{B3}$$

Decomposing the quark self-energies $\Sigma_{ff'}(p)$ with respect to their spinorial structure,

$$\Sigma_{ff'}(p) = \Sigma^L_{ff'}(p^2) \not{p} P_L + \Sigma^R(p^2) \not{p} P_R + \Sigma^D_{ff'}(p^2) P_L + \Sigma^{D*}_{f'f}(p^2) P_R. \tag{B4}$$

We may rewrite (B3) as follows:

$$\Gamma^{G^0 ff'}(0, p, p) = \frac{ig_w}{M_W} T_z^f [\Sigma^D_{ff'}(p^2) P_L - P_R \Sigma^{D*}_{f'f}(p^2)]. \tag{B5}$$

Considering the proper normalizations determined by the relations given in (3.13), it is possible to make the following identifications in the effective potential limit $p^\mu \to 0$:

$$\begin{aligned} \Sigma^D_{ff'}(0) &= \mathbf{U}_R^{f\dagger} \mathbf{h}_f \langle \mathbf{\Delta}_f \rangle \mathbf{U}_L^f, \\ P_L \Gamma^{G^0 ff'}(0, 0, 0) &= -\frac{i}{\sqrt{2}} \mathbf{U}_R^{f\dagger} \mathbf{h}_f \mathbf{\Delta}_f^{G^0} \mathbf{U}_L^f P_L, \end{aligned} \tag{B6}$$

where the unitary matrices $\mathbf{U}_{L,R}^{u,d}$ take care of the weak to the mass basis transformations as given in (3.7), with $\mathbf{U}_L^u = \mathbf{U}_L^Q$ and $\mathbf{U}_L^d = \mathbf{U}_L^Q \mathbf{V}$. Then, the simplified WI (B5) implies that

$$\mathbf{\Delta}_f^{G^0} = -\frac{\sqrt{2}}{v} T_z^f \langle \mathbf{\Delta}_f \rangle, \tag{B7}$$

which is the relation assumed in Sec. III [cf. (3.17)].

We now turn our attention to the WI involving the W^+ boson and the associated would-be Goldstone boson G^+. In the effective potential limit q^μ, $p^\mu \to 0$, we obtain

$$i\Gamma^{G^+ ud}(0, 0, 0) = -\frac{ig_w}{\sqrt{2} M_W} [\mathbf{V}_{u'd} \Sigma^D_{uu'}(0) P_L - \mathbf{V}_{ud'} \Sigma^{D*}_{d'd}(0) P_R]. \tag{B8}$$

Employing the definitions (3.13) and taking the weak-to-mass basis rotations of the quark states into account, we find the relations:

$$\begin{aligned} P_L \Gamma^{G^+ ud}(0, 0, 0) &= \mathbf{U}_R^{u\dagger} \mathbf{h}_u \mathbf{\Delta}_u^{G^+} \mathbf{U}_L^d P_L, \\ P_L \Gamma^{G^- du}(0, 0, 0) &= \mathbf{U}_R^{d\dagger} \mathbf{h}_d \mathbf{\Delta}_d^{G^-} \mathbf{U}_L^u P_L. \end{aligned} \tag{B9}$$

From the simplified WI (B8) and its Hermitian conjugate, we then derive that

$$\mathbf{\Delta}_u^{G^+} = -\frac{\sqrt{2}}{v} \langle \mathbf{\Delta}_u \rangle, \qquad \mathbf{\Delta}_d^{G^-} = \frac{\sqrt{2}}{v} \langle \mathbf{\Delta}_d \rangle, \tag{B10}$$

which is in agreement with (3.17) and the discussion given below. We note that the unitarity of the radiatively corrected CKM matrix $\mathbf{V}$ lies at the heart of deriving the relations (B7) and (B10).

APPENDIX C: `CPsuperH` INTERFACE

To solve the RGEs given in Appendix A, we have considered the following input parameters:

(i) The gauge couplings at the scale M_Z:

$$\alpha_1(M_Z) = \frac{5}{3} \frac{g'^2(M_Z)}{4\pi}; \qquad \alpha_2(M_Z) = \frac{g^2(M_Z)}{4\pi}; \qquad \alpha_3(M_Z), \tag{C1}$$

where $g(M_Z) = e(M_Z)/s_W$ and $g'(M_Z) = e(M_Z)/c_W$ with $\alpha_{\rm em}(M_Z) = e^2(M_Z)/4\pi$.
The evolutions of $\alpha_{1,2}$ from M_Z to $m_t^{\rm pole}$ are determined by [57]

$$\begin{aligned} \alpha_1^{-1}(m_t^{\rm pole}) &= \alpha_1^{-1}(M_Z)^{-1} + \frac{53}{30\pi} \ln(M_Z/m_t^{\rm pole}), \\ \alpha_2^{-1}(m_t^{\rm pole}) &= \alpha_2^{-1}(M_Z) - \frac{11}{6\pi} \ln(M_Z/m_t^{\rm pole}). \end{aligned} \tag{C2}$$

On the other hand, $\alpha_3(m_t^{\rm pole})$ has been obtained by solving the following equation iteratively [58]

$$\alpha_3^{-1}(m_t^{\rm pole}) = \alpha_3^{-1}(M_Z) - b_0 \ln\left(\frac{m_t^{\rm pole}}{M_Z}\right) - \frac{b_1}{b_0} \times \ln\left(\frac{\alpha_3(m_t^{\rm pole})}{\alpha_3(M_Z)}\right) - \left(\frac{b_2 b_0 - b_1^2}{b_0^2}\right) \times [\alpha_3(m_t^{\rm pole}) - \alpha_3(M_Z)] + \mathcal{O}(\alpha_3^2), \tag{C3}$$

where $b_0 = -(11 - 2N_F/3)/2\pi$, $b_1 = -(51 - 19N_F/3)/4\pi^2$, and $b_2 = -(2857 - 5033N_F/9 + 325N_F^2/27)/64\pi^3$ with $N_F = 5$.

(ii) The masses of the quarks and the charged leptons at the top-quark pole-mass scale $m_t^{\rm pole}$. In particular, the top-quark running mass at $m_t^{\rm pole}$ is obtained from: $m_t(m_t^{\rm pole}) = m_t^{\rm pole}/[1 + 4\alpha_3(m_t^{\rm pole})/3\pi]$. The CKM matrix $\mathbf{V}$ is assumed to be given at the same scale $m_t^{\rm pole}$. Then, in general, the complex 3×3 Yukawa matrices at $m_t^{\rm pole}$ are given by

$$\mathbf{h}_{u,e}(m_t^{\rm pole}) = \frac{\sqrt{2}}{v}\hat{\mathbf{M}}_{u,e}(m_t^{\rm pole}),$$
$$\mathbf{h}_{d}(m_t^{\rm pole}) = \frac{\sqrt{2}}{v}\hat{\mathbf{M}}_{d}(m_t^{\rm pole})\mathbf{V}^\dagger(m_t^{\rm pole}) \quad \text{(C4)}$$

in the flavor basis $\mathbf{U}_L^Q = \mathbf{U}_R^u = \mathbf{U}_R^d = \mathbf{1}_3$. The diagonal quark and charged-lepton mass matrices are given by

$$\hat{\mathbf{M}}_u(m_t^{\rm pole}) = \mathbf{diag}[m_u(m_t^{\rm pole}), m_c(m_t^{\rm pole}), m_t(m_t^{\rm pole})],$$
$$\hat{\mathbf{M}}_d(m_t^{\rm pole}) = \mathbf{diag}[m_d(m_t^{\rm pole}), m_s(m_t^{\rm pole}), m_b(m_t^{\rm pole})],$$
$$\hat{\mathbf{M}}_e(m_t^{\rm pole}) = \mathbf{diag}[m_e(m_t^{\rm pole}), m_\mu(m_t^{\rm pole}), m_\tau(m_t^{\rm pole})]. \quad \text{(C5)}$$

Given $\alpha_{1,2,3}(m_t^{\rm pole})$ and $\mathbf{h}_{u,d,e}(m_t^{\rm pole})$, the evolution from $m_t^{\rm pole}$ to the scale $M_{\rm SUSY}$ has been obtained by solving the SM RGEs. Here the SUSY scale $M_{\rm SUSY}$ has been determined by solving

$$Q^2|_{Q=M_{\rm SUSY}} = \max[m_{\tilde{t}}^2(Q^2), m_{\tilde{b}}^2(Q^2)] \quad \text{(C6)}$$

iteratively, where $m_{\tilde{t}}^2 \equiv \max(m_{\tilde{Q}_3}^2 + m_t^2, m_{\tilde{U}_3}^2 + m_t^2)$ and $m_{\tilde{b}}^2 \equiv \max(m_{\tilde{Q}_3}^2 + m_b^2, m_{\tilde{D}_3}^2 + m_b^2)$. For $m_{\tilde{Q}_3,\tilde{U}_3,\tilde{D}_3,\tilde{L}_3,\tilde{E}_3}^2(Q^2)$, we have taken the (3, 3) component of the corresponding mass matrix as

$$m_{\tilde{Q}_3,\tilde{U}_3,\tilde{D}_3,\tilde{L}_3,\tilde{E}_3}^2(Q^2) = [\tilde{\mathbf{M}}_{Q,U,D,L,E}^2(Q^2)]_{(3,3)}. \quad \text{(C7)}$$

At the scale $M_{\rm SUSY}$, the Yukawa matrices match as

$$\mathbf{h}_u(M_{\rm SUSY}^+) = \mathbf{h}_u(M_{\rm SUSY}^-)/\sin\beta(M_{\rm SUSY}),$$
$$\mathbf{h}_{d,e}(M_{\rm SUSY}^+) = \mathbf{h}_{d,e}(M_{\rm SUSY}^-)/\cos\beta(M_{\rm SUSY}), \quad \text{(C8)}$$

and, finally, the evolution from $M_{\rm SUSY}$ to $M_{\rm GUT}$ have been obtained by solving the MSSM RGEs.

(iii) The 19 flavor-singlet mass scales of the MSSM with MCPMFV, which are parametrized as follows:

$$|M_{1,2,3}|e^{i\Phi_{1,2,3}}, \quad |A_{u,d,e}|e^{i\Phi_{A_{u,d,e}}}, \quad \tilde{M}_{Q,U,D,L,E}^2, \quad M_{H_{u,d}}^2. \quad \text{(C9)}$$

These are inputted at the GUT scale $M_{\rm GUT}$, which is defined as the scale where the couplings g_1 and g_2 meet. Any difference between $g_3(M_{\rm GUT})$ and $g_1(M_{\rm GUT})$ may be attributed to some unknown threshold effect at the GUT scale.

By solving the RGEs from the GUT scale $M_{\rm GUT}$ to the SUSY scale $M_{\rm SUSY}$, we obtain:

(i) Three complex gaugino masses, $|M_i|e^{i\Phi_i}(Q = M_{\rm SUSY})$.

(ii) Three 3×3 complex Yukawa-coupling matrices, $\mathbf{h}_{u,d,e}(Q = M_{\rm SUSY})$.

(iii) Three 3×3 complex **a**-term matrices, $\mathbf{a}_{u,d,e}(Q = M_{\rm SUSY})$.

(iv) The soft Higgs masses, $M_{H_u,H_d}^2(Q = M_{\rm SUSY})$.

(v) The complex 3×3 sfermion mass matrices, $\tilde{\mathbf{M}}_{Q,U,D,L,E}^2(Q = M_{\rm SUSY})$.

The inputs for the code `CPsuperH` are:

$$\tan\beta(m_t^{\rm pole}), \quad M_{H^\pm}^{\rm pole}, \quad \mu(M_{\rm SUSY}),$$
$$M_{1,2,3}(M_{\rm SUSY}), \quad m_{\tilde{Q}_3,\tilde{U}_3,\tilde{D}_3,\tilde{L}_3,\tilde{E}_3}(M_{\rm SUSY}), \quad \text{(C10)}$$
$$A_t(M_{\rm SUSY}), \quad A_b(M_{\rm SUSY}), \quad A_\tau(M_{\rm SUSY}).$$

The ratio of the vacuum expectation values at $m_t^{\rm pole}$ is related to that at $M_{\rm SUSY}$ by [21]

$$\tan\beta(m_t^{\rm pole}) = \frac{\xi_2^-(m_t^{\rm pole})}{\xi_1^+(m_t^{\rm pole})}\tan\beta(M_{\rm SUSY}) \quad \text{(C11)}$$

with

$$\xi_{1(2)}^{+(-)}(m_t^{\rm pole}) = 1 + \frac{3|h_{b(t)}|^2}{32\pi^2}\ln\frac{M_{\rm SUSY}^2}{m_t^{\rm pole2}}. \quad \text{(C12)}$$

The gaugino mass parameters are directly read from the results of the RG running, the sfermion masses are given by

$$m_{\tilde{Q}_3,\tilde{U}_3,\tilde{D}_3,\tilde{L}_3,\tilde{E}_3}(M_{\rm SUSY}) = \{[\tilde{\mathbf{M}}_{Q,U,D,L,E}^2(M_{\rm SUSY})]_{(3,3)}\}^{1/2}, \quad \text{(C13)}$$

and the A parameters, including their CP-violating phases, by

$$A_f(M_{\rm SUSY}) = \frac{[\mathbf{a}_f(M_{\rm SUSY})]_{(3,3)}}{[\mathbf{h}_f(M_{\rm SUSY})]_{(3,3)}}. \quad \text{(9.14)}$$

The μ parameter and charged-Higgs-boson pole mass $M_{H^\pm}^{\rm pole}$ can be obtained from $M_{H_u}^2(M_{\rm SUSY})$ and $M_{H_d}^2(M_{\rm SUSY})$ by imposing the two CP-even tadpole conditions, $T_{\phi_1} = T_{\phi_2} = 0$ [21]. The tadpoles can be cast into the form

$$T_{\phi_1(\phi_2)} = v_{1(2)}\bar{\mu}_{1(2)}^2 + v_{2(1)}\,{\rm Re}\bar{m}_{12}^2 + v_{1(2)}[\bar{\lambda}_{1(2)}v_{1(2)}^2 + \tfrac{1}{2}(\bar{\lambda}_3 + \bar{\lambda}_4)v_{2(1)}^2] + v_{1(2)}X_{1(2)}, \quad \text{(C15)}$$

where

$$X_{1(2)} \equiv \frac{3}{8\pi^2}\left[|h_{b(t)}|^2 m_{b(t)}^2\left(\ln\frac{m_{b(t)}^2}{m_t^{\rm pole2}} - 1\right)\right]. \quad \text{(C16)}$$

The quantities $\bar{\mu}_{1,2}^2$ and $\bar{\lambda}_i$ are given by

$$\bar{\mu}_{1,2}^2 = -M_{H_d,H_u}^2 - |\mu|^2 + \mu_{1,2}^{2(1)}(m_t^{\rm pole}),$$
$$\bar{\lambda}_i = \lambda_i + \lambda_i^{(1)}(m_t^{\rm pole}) + \lambda_i^{(2)}(m_t^{\rm pole}), \quad \text{(C17)}$$

where

$$\mu_1^{2(1)}(m_t^{\rm pole}) = -\frac{3}{16\pi^2}\left[|h_t|^2|\mu|^2 \ln\frac{M_{\tilde{t}}^2}{m_t^{\rm pole2}} + |h_b|^2|A_b|^2 \ln\frac{M_{\tilde{b}}^2}{m_t^{\rm pole2}}\right],$$
$$\mu_2^{2(1)}(m_t^{\rm pole}) = -\frac{3}{16\pi^2}\left[|h_t|^2|A_t|^2 \ln\frac{M_{\tilde{t}}^2}{m_t^{\rm pole2}} + |h_b|^2|\mu|^2 \ln\frac{M_{\tilde{b}}^2}{m_t^{\rm pole2}}\right]. \quad \text{(C18)}$$

The couplings λ_i, $\lambda_i^{(1)}(m_t^{\rm pole})$ and $\lambda_i^{(2)}(m_t^{\rm pole})$ may be found in Ref. [21]. The squared absolute value $|\mu|^2$ can be determined from $(T_{\phi_1}/v_2 - T_{\phi_2}/v_1) = 0$, which does not depend on $\mathrm{Re}\,\bar{m}_{12}^2$, since

$$|\mu|^2 = \frac{(M_{H_d}^2 - M_{H_u}^2 t_\beta^2) - (\bar{\lambda}_1 v_1^2 - \bar{\lambda}_2 v_2^2 t_\beta^2) + X_A - (X_1 - t_\beta^2 X_2)}{(t_\beta^2 - 1) + X_{tb}} \quad \text{(C19)}$$

with

$$X_A \equiv \frac{3}{16\pi^2}\left(|h_b|^2|A_b|^2 \ln\frac{M_{\tilde{b}}^2}{m_t^{\rm pole2}} - t_\beta^2|h_t|^2|A_t|^2 \ln\frac{M_{\tilde{t}}^2}{m_t^{\rm pole2}}\right), \qquad X_{tb} \equiv -\frac{3}{16\pi^2}\left(|h_t|^2 \ln\frac{M_{\tilde{t}}^2}{m_t^{\rm pole2}} - t_\beta^2|h_b|^2 \ln\frac{M_{\tilde{b}}^2}{m_t^{\rm pole2}}\right). \quad \text{(C20)}$$

We note that the phase of the μ parameter, Φ_μ, is not renormalized.

Once $|\mu|^2$ is found, $\mathrm{Re}\,\bar{m}_{12}^2$ can be obtained from $T_{\phi_1} = 0$ or $T_{\phi_2} = 0$. With $\mathrm{Re}\,\bar{m}_{12}^2$ known, the charged-Higgs-boson pole mass can be obtained by solving the following equation iteratively:

$$(M_{H^\pm}^{\rm pole})^2 = \frac{\mathrm{Re}\,\bar{m}_{12}^2}{s_\beta c_\beta} + \frac{1}{2}\bar{\lambda}_4 v^2 - \mathrm{Re}\,\hat{\Pi}_{H^+H^-}(\sqrt{s} = M_{H^\pm}^{\rm pole}). \quad \text{(C21)}$$

For the explicit form of $\hat{\Pi}_{H^+H^-}$, we refer to Ref. [59]. We note that, for large $\tan\beta$, $\mathrm{Re}\,\bar{m}_{12}^2/s_\beta c_\beta \simeq M_{H_d}^2 - M_{H_u}^2 - M_Z^2$ at the tree level. Finally, after imposing the *CP*-odd tadpole condition $\mathrm{Im}(B\mu) = 0$, we use $B\mu = \mathrm{Re}\,\bar{m}_{12}^2$ to calculate the 2HDM contribution (3.28), by noting $H_u H_d = -\Phi_1^\dagger \Phi_2$.

[1] S. L. Glashow, J. Iliopoulos, and L. Maiani, Phys. Rev. D **2**, 1285 (1970).

[2] N. Cabibbo, Phys. Rev. Lett. **10**, 531 (1963); M. Kobayashi and T. Maskawa, Prog. Theor. Phys. **49**, 652 (1973).

[3] T. Banks, Nucl. Phys. **B303**, 172 (1988); E. Ma, Phys. Rev. D **39**, 1922 (1989).

[4] R. Hempfling, Phys. Rev. D **49**, 6168 (1994); L. J. Hall, R. Rattazzi, and U. Sarid, Phys. Rev. D **50**, 7048 (1994); T. Blazek, S. Raby, and S. Pokorski, Phys. Rev. D **52**, 4151 (1995); M. Carena, M. Olechowski, S. Pokorski, and C. E. M. Wagner, Nucl. Phys. **B426**, 269 (1994); F. Borzumati, G. Farrar, N. Polonsky, and S. Thomas, Nucl. Phys. **B555**, 53 (1999).

[5] M. Carena, D. Garcia, U. Nierste, and C. E. Wagner, Nucl. Phys. **B577**, 88 (2000).

[6] C. S. Huang and Q.-S. Yan, Phys. Lett. B **442**, 209 (1998); S. R. Choudhury and N. Gaur, Phys. Lett. B **451**, 86 (1999); C. S. Huang, W. Liao, and Q.-S. Yan, Phys. Rev. D **59**, 011701 (1998); C. Hamzaoui, M. Pospelov, and M. Toharia, Phys. Rev. D **59**, 095005 (1999); K. S. Babu and C. Kolda, Phys. Rev. Lett. **84**, 228 (2000); G. Isidori and A. Retico, J. High Energy Phys. 11 (2001) 001; A. Dedes, H. K. Dreiner, and U. Nierste, Phys. Rev. Lett. **87**, 251804 (2001).

[7] P. H. Chankowski and Lucja Slawianowska, Phys. Rev. D **63**, 054012 (2001); C. S. Huang, W. Liao, Q.-S. Yan, and S.-H. Zhu, Phys. Rev. D **63**, 114021 (2001).

[8] C. Bobeth, T. Ewerth, F. Krüger, and J. Urban, Phys. Rev. D **64**, 074014 (2001).

[9] R. Arnowitt, B. Dutta, T. Kamon, and M. Tanaka, Phys. Lett. B **538**, 121 (2002); S. Baek, P. Ko, and W. Y. Song, J. High Energy Phys. 03 (2003) 054.

[10] G. D'Ambrosio, G. F. Giudice, G. Isidori, and A. Strumia, Nucl. Phys. **B645**, 155 (2002).

[11] A. J. Buras, P. H. Chankowski, J. Rosiek, and L. Slawianowska, Phys. Lett. B **546**, 96 (2002); Nucl. Phys. **B659**, 3 (2003).

[12] A. Dedes and A. Pilaftsis, Phys. Rev. D **67**, 015012 (2003).

[13] T. Ibrahim and P. Nath, Phys. Rev. D **67**, 016005 (2003); M. E. Gomez, T. Ibrahim, P. Nath, and S. Skadhauge, Phys. Rev. D **74**, 015015 (2006); T. F. Feng, X. Q. Li, and J. Maalampi, Phys. Rev. D **73**, 035011 (2006).

[14] J. Foster, K. i. Okumura, and L. Roszkowski, J. High Energy Phys. 08 (2005) 094.

[15] M. S. Carena, A. Menon, R. Noriega-Papaqui, A. Szynkman, and C. E. M. Wagner, Phys. Rev. D **74**, 015009 (2006).

[16] A. G. Akeroyd and S. Recksiegel, J. Phys. G **29**, 2311 (2003).

[17] H. Itoh, S. Komine, and Y. Okada, Prog. Theor. Phys. **114**, 179 (2005).

[18] H. G. Evans (CDF Collaboration), arXiv:0705.4598.

[19] A. Pilaftsis, Phys. Rev. D **58**, 096010 (1998); Phys. Lett. B **435**, 88 (1998).

[20] For example, see, S. Antusch, S. F. King, and M. Malinsky, arXiv:0708.1282.

[21] M. Carena, J. Ellis, A. Pilaftsis, and C. E. M. Wagner, Nucl. Phys. **B586**, 92 (2000).

[22] S. R. Coleman and E. Weinberg, Phys. Rev. D **7**, 1888 (1973).

[23] A. Pilaftsis and C. E. M. Wagner, Nucl. Phys. **B553**, 3 (1999); D. A. Demir, Phys. Rev. D **60**, 055006 (1999); S. Y. Choi, M. Drees, and J. S. Lee, Phys. Lett. B **481**, 57 (2000); G. L. Kane and L.-T. Wang, Phys. Lett. B **488**, 383 (2000); T. Ibrahim and P. Nath, Phys. Rev. D **63**, 035009 (2001); **66**, 015005 (2002); S. Y. Choi, K. Hagiwara, and J. S. Lee, Phys. Rev. D **64**, 032004 (2001); S. Heinemeyer, Eur. Phys. J. C **22**, 521 (2001); M. Carena, J. Ellis, A. Pilaftsis, and C. E. M. Wagner, Nucl. Phys. **B625**, 345 (2002); M. Boz, Mod. Phys. Lett. A **17**, 215 (2002); S. W. Ham, S. K. Oh, E. J. Yoo, C. M. Kim, and D. Son, Phys. Rev. D **68**, 055003 (2003); M. Frank, T. Hahn, S. Heinemeyer, W. Hollik, H. Rzehak, and G. Weiglein, J. High Energy Phys. 02 (2007) 047.

[24] A. Pilaftsis, Phys. Lett. B **422**, 201 (1998); D. Binosi, J. Papavassiliou, and A. Pilaftsis, Phys. Rev. D **71**, 085007 (2005).

[25] J. R. Ellis, M. K. Gaillard, and D. V. Nanopoulos, Nucl. Phys. **B106**, 292 (1976).

[26] J. Ellis, G. Ridolfi, and F. Zwirner, Phys. Lett. B **257**, 83 (1991); Y. Okada, M. Yamaguchi, and T. Yanagida, Phys. Lett. B **262**, 54 (1991); H. E. Haber and R. Hempfling, Phys. Rev. Lett. **66**, 1815 (1991).

[27] A. A. Akhundov, D. Y. Bardin, and T. Riemann, Nucl. Phys. **B276**, 1 (1986); J. Bernabeu, A. Pich, and A. Santamaria, Phys. Lett. B **200**, 569 (1988).

[28] A. J. Buras, S. Jäger, and J. Urban, Nucl. Phys. **B605**, 600 (2001).

[29] M. Ciuchini *et al.*, J. High Energy Phys. 07 (2001) 013.

[30] A. J. Buras, M. Misiak, and J. Urban, Nucl. Phys. **B586**, 397 (2000).

[31] D. Becirevic, V. Gimenez, G. Martinelli, M. Papinutto, and J. Reyes, Nucl. Phys. B, Proc. Suppl. **106**, 385 (2002).

[32] A. J. Buras, P. H. Chankowski, J. Rosiek, and L. Slawianowska, Nucl. Phys. **B619**, 434 (2001).

[33] H. Fusaoka and Y. Koide, Phys. Rev. D **57**, 3986 (1998).

[34] W. S. Hou, Phys. Rev. D **48**, 2342 (1993).

[35] A. L. Kagan and M. Neubert, Phys. Rev. D **58**, 094012 (1998); Eur. Phys. J. C **7**, 5 (1999).

[36] M. Misiak *et al.*, Phys. Rev. Lett. **98**, 022002 (2007).

[37] G. Belanger, F. Boudjema, A. Pukhov, and A. Semenov, Comput. Phys. Commun. **174**, 577 (2006).

[38] M. Ciuchini, G. Degrassi, P. Gambino, and G. F. Giudice, Nucl. Phys. **B527**, 21 (1998).

[39] M. Ciuchini, G. Degrassi, P. Gambino, and G. F. Giudice, Nucl. Phys. **B534**, 3 (1998); G. Degrassi, P. Gambino, and P. Slavich, Phys. Lett. B **635**, 335 (2006).

[40] J. S. Lee, A. Pilaftsis, M. Carena, S. Y. Choi, M. Drees, J. R. Ellis, and C. E. M. Wagner, Comput. Phys. Commun. **156**, 283 (2004).

[41] S. Bertolini, F. Borzumati, A. Masiero, and G. Ridolfi, Nucl. Phys. **B353**, 591 (1991); T. Goto, Y. Okada, Y. Shimizu, and M. Tanaka, Phys. Rev. D **55**, 4273 (1997); **66**, 019901(E) (2002); Y. G. Kim, P. Ko, and J. S. Lee, Nucl. Phys. **B544**, 64 (1999); F. Borzumati, C. Greub, T. Hurth, and D. Wyler, Phys. Rev. D **62**, 075005 (2000).

[42] M. Battaglia *et al.*, Eur. Phys. J. C **22**, 535 (2001); B. C. Allanach *et al.*, arXiv:hep-ph/0202233; N. Ghodbane and H. U. Martyn, arXiv:hep-ph/0201233; M. Battaglia, A. De Roeck, J. R. Ellis, F. Gianotti, K. A. Olive, and L. Pape, Eur. Phys. J. C **33**, 273 (2004).

[43] For a partial list, see, for example, T. Ibrahim and P. Nath, Phys. Rev. D **58**, 111301 (1998); **61**, 093004 (2000); M. Brhlik, G. J. Good, and G. L. Kane, Phys. Rev. D **59**, 115004 (1999); A. Bartl, T. Gajdosik, W. Porod, P. Stockinger, and H. Stremnitzer, Phys. Rev. D **60**, 073003 (1999); T. Falk, K. A. Olive, M. Pospelov, and R. Roiban, Nucl. Phys. **B560**, 3 (1999); D. Chang, W.-Y. Keung, and A. Pilaftsis, Phys. Rev. Lett. **82**, 900 (1999); S. Pokorski, J. Rosiek, and C. A. Savoy, Nucl. Phys. **B570**, 81 (2000); E. Accomando, R. Arnowitt, and B. Dutta, Phys. Rev. D **61**, 115003 (2000).A. Pilaftsis, Nucl. Phys. **B644**, 263 (2002).For recent compilations of the experimental constraints, see, V. D. Barger, T. Falk, T. Han, J. Jiang, T. Li, and T. Plehn, Phys. Rev. D **64**, 056007 (2001); K. A. Olive, M. Pospelov, A. Ritz, and Y. Santoso, Phys. Rev. D **72**, 075001 (2005); J. R. Ellis, J. S. Lee, and A. Pilaftsis, Mod. Phys. Lett. A **21**, 1405 (2006).

[44] T. Goto, Y. Y. Keum, T. Nihei, Y. Okada, and Y. Shimizu, Phys. Lett. B **460**, 333 (1999).

[45] W. M. Yao *et al.* (Particle Data Group), J. Phys. G **33**, 1 (2006).

[46] K. Ikado *et al.*, Phys. Rev. Lett. **97**, 251802 (2006).

[47] B. Aubert (The *BABAR* Collaboration), Phys. Rev. D **76**, 052002 (2007).

[48] M. Bona *et al.* (UTfit Collaboration), J. High Energy Phys. 10 (2006) 081.

[49] G. Isidori, F. Mescia, P. Paradisi, and D. Temes, Phys. Rev. D **75**, 115019 (2007).

[50] E. Barberio *et al.* (Heavy Flavor Averaging Group (HFAG) Collaboration), arXiv:0704.3575.

[51] B. Grzadkowski, M. Lindner, and S. Theisen, Phys. Lett. B **198**, 64 (1987); S. Antusch, J. Kersten, M. Lindner, and M. Ratz, Phys. Lett. B **538**, 87 (2002).

[52] V. Barger, M. S. Berger, and P. Ohmann, Phys. Rev. D **49**, 4908 (1994).

[53] D. J. Castano, E. J. Piard, and P. Ramond, Phys. Rev. D **49**, 4882 (1994).

[54] See, for instance, A. Pilaftsis, Phys. Rev. D **65**, 115013 (2002).

[55] J. M. Cornwall and J. Papavassiliou, Phys. Rev. D **40**, 3474 (1989); J. Papavassiliou, Phys. Rev. D **41**, 3179 (1990); D. Binosi and J. Papavassiliou, Phys. Rev. D **66**, 111901 (2002); J. Phys. G **30**, 203 (2004).

[56] M. Binger and S. J. Brodsky, Phys. Rev. D **74**, 054016 (2006); N. Caporaso and S. Pasquetti, arXiv:hep-th/0609168.

[57] V. D. Barger, M. S. Berger, and P. Ohmann, Phys. Rev. D **47**, 1093 (1993).

[58] W. J. Marciano, Phys. Rev. D **29**, 580 (1984).

[59] M. Carena, J. Ellis, A. Pilaftsis, and C. E. M. Wagner in Ref. [23].